

79  
NACA TN 3062

TECH LIBRARY KAFB, NM  
0066294

# NATIONAL ADVISORY COMMITTEE FOR AERONAUTICS

## TECHNICAL NOTE 3062

A FLIGHT INVESTIGATION OF THE PRACTICAL  
PROBLEMS ASSOCIATED WITH POROUS-  
LEADING-EDGE SUCTION

By Paul A. Hunter and Harold I. Johnson

Langley Aeronautical Laboratory  
Langley Field, Va.



Washington  
February 1954

AFMDC  
TECHNICAL LIBRARY  
AFL 2011



---

TECHNICAL NOTE 3062

---

A FLIGHT INVESTIGATION OF THE PRACTICAL  
PROBLEMS ASSOCIATED WITH POROUS-  
LEADING-EDGE SUCTION

By Paul A. Hunter and Harold I. Johnson

SUMMARY

A flight investigation has been made of the practical problems associated with the use of porous-leading-edge suction. The wing leading edge of the test airplane was porous over approximately 83 percent of the span and the first 8 percent of the chord on the upper surface. Various other extents of suction area within these limits were also tested.

Results of this investigation have indicated that a wing equipped with porous-leading-edge suction can be constructed which has sufficient strength and durability for use in flight without adding excessive weight. For the type of porous material used in this investigation, clogging due to atmospheric dust did not appear to be a problem. For the light rain encountered in flight, the power required to produce a given flow coefficient was about 50 percent more than that required for the dry condition. Based on the ground data, it was estimated that for flight in heavy rain the power would be approximately twice that for the dry condition. At maximum blower speed the porous area became cleared within 3 to 4 minutes after water ceased to impinge on the surface. Under certain conditions, tests showed a severe vibration of the porous material induced by an "organ pipe" resonance of the air column within the ducts. As expected from wind-tunnel results obtained previous to this investigation, the use of leading-edge suction with the small amount of power available had little effect on the maximum lift coefficient developed with the airfoil section used in this wing (NACA 2412). In general, an appreciable drop occurred in maximum lift coefficient from the leading-edge-sealed configuration to the condition of zero suction with the porous-area configurations tested. Increments in lift coefficient due to the suction available generally brought the maximum lift coefficient back approximately to the value for the wing with the leading edge sealed. The maximum theoretical aerodynamic power, if duct losses are excluded, varied with the configurations tested from 3.65 to 9.70 horsepower.

## INTRODUCTION

The use of porous surfaces for boundary-layer control has for a period of approximately 30 years been the subject of many theoretical and experimental studies involving area suction. Previous flight studies of area suction have been limited mostly to models and partial-span test sections (for example, refs. 1 and 2), although an incomplete investigation of area suction applied to nearly all the rearward portions of the upper surface of the wings of an airplane was made in England near the beginning of World War II (ref. 3). In the present investigation, porous-leading-edge area suction covering the first 8 percent chord on the upper surface was applied to essentially the entire wing span of the airplane tested.

The use of area suction involves several practical problems which are not readily solvable by wind-tunnel studies. One of the general problems is the clogging of the pores of the more dense materials by atmospheric dust and by rain. Construction of a structurally efficient wing with porous surfaces is another practical problem which, though important, does not appear to be extremely difficult, particularly in the design of a new wing where the ducting can be made part of the load-carrying structure.

The National Advisory Committee for Aeronautics has conducted a flight-test program to investigate various practical problems associated with the use of porous materials for boundary-layer control. Because the airplane available for the tests had a rounded-leading-edge type of airfoil (NACA 2412) characterized by a trailing-edge stall, very little benefit in maximum lift could be expected from the application of leading-edge suction. This expectation was verified by two-dimensional wind-tunnel tests made prior to the flight investigation.

## SYMBOLS

b span, ft

c local chord, ft

$C_L$  airplane lift coefficient,  $\frac{W}{q_c S_A} (n \cos \alpha + l \sin \alpha)$

|            |   |
|------------|---|
| $C_Q$      | suction flow coefficient (a constant value of $S_A'$ corresponding to 89.2 percent of total wing area was used in computing flow coefficients), $\frac{Q}{VS_A'}$ |
| $H_O$      | free-stream total pressure, $q_c + p_o$ , lb/sq ft  |
| $H_d$      | duct total pressure, $p_d + q_d$ , lb/sq ft   |
| $H_1$      | duct total pressure at outboard measuring station, lb/sq ft<br>(assumed $H_1 = p_1$ ; $q_1 = 0$ )   |
| $l$        | longitudinal acceleration, positive forward, g units  |
| $n$        | normal acceleration, positive upward, g units   |
| $p$        | static pressure at wing surface, lb/sq ft   |
| $p_o$      | free-stream static pressure, lb/sq ft   |
| $p_d$      | duct static pressure at inboard measuring station, lb/sq ft   |
| $p_1$      | duct static pressure at outboard measuring station, lb/sq ft  |
| $\Delta p$ | pressure difference across porous material, lb/sq ft  |
| $Q$        | total volume flow rate, cu ft/sec   |
| $q$        | impact pressure at wing surface, lb/sq ft   |
| $q_c$      | calibrated impact pressure, lb/sq ft  |
| $q_d$      | duct impact pressure at inboard measuring station, lb/sq ft   |
| $q_1$      | duct impact pressure at outboard measuring station, lb/sq ft  |
| $S$        | pressure coefficient, $\frac{H_O - p}{q_c} = \frac{q}{q_c}$   |
| $S_A$      | wing area, sq ft  |
| $S_A'$     | wing area affected by suction (area between spanwise stations at outer extents of porous area)  |
| $S_p$      | area of porous material measured along surface, sq ft   |

|          |   |
|----------|---|
| V        | true airspeed, ft/sec   |
| v        | apparent velocity through porous material, $\frac{Q}{S_p}$ , ft/sec |
| W        | airplane weight, lb   |
| x        | chordwise distance, ft  |
| y        | spanwise distance, ft   |
| z        | distance normal to airfoil chord, ft                                |
| $\alpha$ | calibrated angle of attack referred to thrust axis, deg             |

#### APPARATUS

##### Airplane

Flight tests were conducted on the Cessna 190 airplane (see table I for dimensional data) shown in the photographs presented as figures 1(a) and 1(b) and in the three-view drawing in figure 1(c). The relative size and location of the lower-surface split-type flap are shown in figure 1(c). Figure 1(d) shows a comparison of the actual wing profile at a representative spanwise station with the NACA 2412 profile and also some details of the porous-leading-edge construction to be described subsequently. The actual wing profile differs from the NACA 2412 profile in that it has a slightly larger leading-edge radius, has less camber in the first 10 percent of the chord, and has a slight amount of negative camber in the first 2 percent of the chord. These variations resulted from manufacturing and modification-shop tolerances.

##### Boundary-Layer-Control Equipment

The porous surface consisted of a sandwich containing an outer surface of woven Monel filter cloth, a 16-mesh copper window-screen separator, and a backing of 0.016-inch-thick perforated brass sheet. The filter cloth was woven in Dutch weave with 30 wires by 250 wires per inch to a thickness of 0.028 inch, rolled to 0.020 inch, and further hammered to 0.018 inch to reduce the porosity and improve the surface smoothness. The filter cloth was obtained from the Michigan Wire Cloth Company. The perforated brass, which was used to stiffen the filter cloth, had 714 openings of 0.020-inch diameter per square inch spaced 0.041 inch apart. The sandwich was formed to the leading-edge curvature on steel jigs and the three layers cemented together with a plastic adhesive at the edges only.

Wind-tunnel data indicated that most of the advantage of porous-leading-edge suction on the NACA 2412 airfoil could be obtained with a value of  $C_Q$  of 0.002 which corresponds to an inflow velocity of 3.6 fps at an airspeed of 63 mph. The design porosity was such that a pressure difference of 72.8 lb/sq ft would produce a velocity of 3.6 fps through the porous material. The arithmetic mean of 20 readings of porosity of only the filter cloth showed a velocity 3 percent above design velocity at design pressure difference (more porous). The copper screen and perforated brass do not appear to add appreciable resistance.

Figure 2(a) shows the general arrangement of equipment and ducting in the airplane. The leading edge of the wing was porous over 83.4 percent of the span and the first 8 percent of the chord on the upper surface as shown in figure 1(b). The leading-edge duct was formed by the incorporation of a false spar, duct bottom, and porous material supports as shown in figure 2(b). The porous covering was attached at the edges in sections with machine screws; the edges were faired with modeling clay and shellacked, as shown in figure 2(c). A portion of the window over the pilot's head was replaced by a pan covered with porous material, as shown in figure 1(b), in order to continue the area suction over the center section. The underside of the pan and part of the ducting are shown in figure 2(d). The flow was removed from each wing-leading-edge duct at the wing root by the duct shown in figure 2(e) which incorporated turning vanes in the 90° bend; the flow was then further ducted to the blower as shown in figure 2(f). The small duct shown in figure 2(f) is the continuation of the duct from the center section shown in figure 2(d). From the blower exit, the flow was split and was expelled from the exit holes on the side of the fuselage as shown in figures 1(a) and 2(a). Two butterfly-type shutters were installed in the exit ducts behind the blower.

The blower shown in figure 2(f) is the compressor stage of a large aircraft-engine turbosupercharger which, though not ideally suited to this application, was used because it was readily available. The blower was driven by a small automotive engine rated 25 horsepower at 4,400 rpm and a right-angle gearbox in such a manner that the blower speed was three times that of the engine. The engine-blower installation is shown in figure 2(g). Engine and exit-duct shutter controls were mounted on the top of the engine cover as can be seen in this figure. The louvers in the top of the fuselage just behind the wing, shown in figure 1(c), were installed to remove engine fumes from the cabin.

During the investigation, large deflections of the porous surface occurred when suction was applied in configurations where large portions of the porous area were sealed. This condition required additional stiffeners to reduce the unsupported length of the porous material from the approximately 30-inch spanwise increments shown in figure 2(b) to

about 10 inches. These additional supports were made of thin duralumin placed edgewise to the porous material with the edge sharpened to reduce interference of the support to the flow. The supports were 1 inch wide normal to the wing surface and had the lower edge flanged to stiffen the support and to assist the flow to turn inboard after passing through the porous material. Photographs of the normal leading edge and leading edge buckled by suction are shown in figure 3.

### Instrumentation

Standard NACA instrumentation was provided to record continuously airspeed, three components of acceleration, rolling and pitching velocities, sideslip angle, angle of attack, control positions, control forces, temperatures, angle of bank or pitch, airplane heading, and pressures. The airspeed used in this paper is calibrated airspeed as obtained by measuring pressures from a total-pressure tube and a swivel static-pressure tube mounted on a boom  $1\frac{1}{4}$  chords ahead of the leading edge of the right wing (fig. 1) and by correcting those pressures for position error as determined from a trailing bomb. The angle of attack and angle of sideslip were obtained by use of free-floating vanes mounted on a boom  $1\frac{1}{4}$  chords ahead of the leading edge of the left wing (fig. 1(a)). The angles read from the angle-of-attack vane were corrected for rolling and pitching velocities and error due to the induced flow field ahead of the airplane.

Static pressures were measured at three spanwise positions along the rearward wall, at one position on the outboard end wall of one leading-edge duct, and at one position in the blower exit duct. The orifice on the outboard end wall is referred to subsequently as the outboard measuring station. Flow quantities were measured in each of the three longitudinal ducts by using total pressure and the average of four static pressures in each of the large ducts and by using static pressure at the entry and throat of a venturi in the center-section duct. Temperatures of the flow in one of the large ducts and in the center-section duct were also recorded. A survey of total pressure was made across each main duct prior to the flight tests to determine the velocity distribution in these ducts. A discharge coefficient, estimated at 0.974, was used in determining the velocity through the venturi in the center-section duct.

Tuft pictures of the flow over the wing were made with a rearward-facing 35-millimeter motion-picture camera which was mounted above and behind the wing on the structure shown in figures 1(b) and 2(c) and which photographed a spherical mirror that reflected an image of the entire wing.

## TESTS

Flight tests were made to determine the power requirements, the effect of varying suction flow, and the effect of varying the extent of porous area on the lift coefficient and angle of attack at the stall in the course of accumulating flight time on the porous surfaces. Stalls were made at four different blower speeds in each of the following conditions: airplane engine with a manifold pressure of 25 inches of mercury, at 2,200 rpm, flaps up and down, and airplane engine idling, flaps up and down. All flight data presented in this report were obtained after the additional chordwise stiffeners were installed. In making the flight tests, the blower was set at a predetermined speed at a flight speed of approximately 85 to 90 mph and no further changes in blower control setting were made during the subsequent stall approach. The result was approximately constant-volume flow through the range of airspeed obtained during each test. The various spanwise and chordwise extents of suction tested are shown graphically in figure 4. The extent of porous area was varied by sealing portions of the porous area with cellulose tape. The ratio of wing area affected by suction to total wing area as determined by the spanwise extent of porous area and the ratio of porous area to total wing area are also given. In order to determine the effect of water on the porous material, one flight was made with leading-edge configuration (a) (fig. 4) in rain of varying intensity.

Tests were made on the ground at various times during the program to determine the relative porosity and power requirements of the porous surface as affected by time, flight time, and water. These tests were made by running the blower at various steady rotational speeds. Rain was simulated in some of these ground tests by spraying the wing with water and taking records at full throttle and also by first wetting the wing and then starting the blower engine at full throttle. All ground tests were made with leading-edge configuration (a) (full 8 percent).

## RESULTS AND DISCUSSION

## Practical Problems

Since this investigation was a research project to determine the practicability of the porous surface, the weight and volume of the components other than the porous surface were not given much consideration so long as they were not excessive. As a result, the weight of the airplane with boundary-layer control was large. An appreciable reduction in weights would have been possible had an airplane been designed especially



for the boundary-layer-control installation and had one of the high-power-to-weight-ratio blower systems now available been used. Weights of the primary components are given in table II.

Porosity.- Data affecting the porosity of the porous leading edge as determined from a number of ground tests are shown in table III. The results of the tests are shown in figure 5 plotted as apparent velocity through the porous material against the pressure difference across the porous material. Comparison of the data of tests 1 and 2 indicates no loss in porosity after approximately 12 hours of flight time and 89 days of being parked in a rather dusty hangar. Dust therefore seems to have no adverse effects on the practicability of this type of porous surface. The apparent gain in porosity between tests 1 and 2 may be taken as an indication of the accuracy of measurement, with the true porosity curve lying somewhere between the two faired curves. The loss of porosity shown by the data of test 3 may be attributed to the retention of adhesive from the cellulose tape, which was used to vary the extent of porous area, after the tape had been removed. Tests made after the first two attempts at cleaning (tests 4 and 5) apparently succeeded only in driving the adhesive deeper into the surface with successive losses in porosity. Later tests (tests 6, 7, and 8) made after additional attempts at cleaning and additional flight time showed slight increases in porosity, but test 9 made near the end of the flight investigation showed an appreciable increase in porosity. No cleaning was attempted between tests 6 and 9. The explanation appears to be that the solvents contained in the adhesive particles dried out and permitted the removal of the residue by air and by air and water mixtures which passed through the porous material during flight and ground tests just previous to test 9.

The shape of the curves in figure 5 gives some indication of the type of flow through the porous material. The straight-line curves having their origins at zero for tests 1, 2, 3, and 9 indicate that the flow through the screen for these tests was mostly viscous. Although straight lines could reasonably be faired through the data for the other tests, extrapolation of the lines did not pass through zero velocity at zero pressure. One set of data for which points in the low velocity and pressure range were available (test 8) shows appreciable curvature in this range, an indication of a transition from mostly viscous to mostly turbulent flow. A seemingly reasonable explanation for this change is that, as the effective porous area was reduced by partial blocking of some of the passages in the porous material, the critical Reynolds number of the flow through the porous material was reached and transition to turbulent flow occurred.

Effects of rain.- The effects of rain, real and simulated, on the porous material are shown in figures 6 and 7. Figure 6 shows a comparison of ground and flight tests where the data for the dry ground test are taken from test 8 (see fig. 5). An explanation for the large difference

in pressure differential between the dry and wet conditions for the ground and flight tests may be that the simulated rain for the ground tests was much heavier than the actual rain encountered in flight. The intercept of the dashed lines for the flight data with the pressure scale represents a reasonable value of the average pressure on the external surface of the leading edge in flight as determined by the method explained in the appendix. The pressures for the ground tests represent the pressure difference across the leading edge only, whereas the flight pressures include the pressure drop above the wing (estimated 63 lb/sq ft). Figure 6 shows the increment in pressure produced by simulated heavy rain in ground tests to be approximately equal to the pressure drop above the wing in flight. Thus, for flight in heavy rain the pressure which the blower would have to overcome would be approximately twice that for flight in the dry condition. This increment was of the order of 50 percent for the light rain encountered in flight.

Figure 7 shows a comparison of two ground tests in which the blower engine was started at full throttle. The numbers along the curve represent time in seconds from starting. No water was added to the leading edge for the wet condition after starting. It appears that, under these conditions, the porous material would have completely cleared itself of water within 3 to 4 minutes.

From these results, rain appears to be a very important factor with regard to the practicability of porous-leading-edge suction. A suction system having a blower which operated at design pressure ratio in dry air, as would probably be the case for other than experimental systems, would be greatly hindered in rain, since the blower would not be capable of producing the additional pressure drop necessary to overcome the surface tension of the water in the porous surface. The blower used in this investigation was being operated at pressure ratios of the order of one-fourth its rated pressure ratio; thus, the additional pressure drop was well within its capability inasmuch as the blower efficiency apparently increased greatly with increasing pressure ratio. During the ground simulated rain tests, an appreciable amount of water could be seen coming out of the fuselage exit ducts. This condition would appear to obviate the practicability of using any water-absorbing material such as felt for any part of the porous surface since the water would probably greatly increase the density of the porous surface. Apparently, additional work should be done on the effect of rain on porous-area suction.

Power requirements.- The power requirements were calculated as the product of volume flow rate and difference in total pressure measured at any two stations between which the increment of power was desired. The estimated distribution of power for the gliding condition (aircraft engine idling, flaps up) with leading-edge configuration (a) at maximum blower speed at the stall is shown in figure 8.

Since no wing-surface orifices were provided, the division of the theoretical aerodynamic suction power (called useful power herein for simplicity) into power required to overcome porous-material drag and power required to reduce duct pressure to average surface pressure was calculated. The estimation of the leading-edge surface pressure from which the pressure drop equivalent to these two power requirements was determined is given in the appendix. The maximum theoretical aerodynamic power, if duct losses are excluded, varied with the configurations tested from 3.65 to 9.70 horsepower. The pressure drop proportional to the duct power loss shown in figure 8 was partially measured and partially calculated. Duct loss was measured between the outboard-duct static orifice and the velocity-measuring station in the wing root. Duct losses from this station to the blower and from the blower to the fuselage exits were calculated with the aid of reference 4. The calculated duct loss amounted to about 40 percent of the total duct loss.

The power to drive accessories was estimated to be 1 horsepower and the gearbox efficiency was assumed as 98 percent, which is very reasonable for the spiral bevel gears used. The engine power was taken from a power curve which was supplied by the engine manufacturer with the engine and which was checked and found to be reliable. The blower loss was taken as the difference between the engine power output (at a particular rotational speed) and the total of other power requirements given previously. The maximum obtainable engine rotational speed was appreciably limited by improper matching of engine torque output and torque input required by the blower, so that at no time was full-rated power output of the engine obtained.

Table IV shows the variation with blower speed and leading-edge configuration of the ratio of useful power to engine output power, the ratio of porous-material power to useful power, the approximate ratio of duct power loss to engine output, and the approximate blower efficiency. Values of engine output power and flow coefficient for each case are also given.

#### Aerodynamic Data

Effect of suction on maximum lift.- A summary of the main aerodynamic data obtained during this investigation is shown in figure 9 as the variation of lift coefficient with flow coefficient for various extents of the porous leading edge and various airplane configurations. The first point to be noted is that there is an initial drop in lift coefficient from the completely sealed configuration to the zero-suction case (duct dampers closed) with all leading-edge configurations except configuration (e) (center section only) and configuration (f) (last 1 percent) in figures 9(d) and 9(e), respectively. The apparent reason for this behavior is that a circulatory flow is set up through the porous surface as a

result of the large pressure gradient above the porous area. This circulatory flow evidently has the effect of promoting separation at a lower angle of attack than that at which it would occur if this flow did not exist. Figure 10 shows the theoretical pressure distribution over the upper surface of the leading edge of the NACA 2412 airfoil at a lift coefficient of 1.6. The difference in pressures over the first 1 percent may be seen to be much less than the difference in pressures over the full 8 percent so that there would be less opportunity for local outflow to occur over the first 1 percent. As the chordwise extent of porous area was varied from 8 percent (configuration (a)) in figure 9(a), to 2 percent (configuration (b)) in figure 9(b), and finally to 1 percent (configuration (c)) in figure 9(c), the initial drop in lift coefficient became progressively less. Figure 10 shows that the maximum difference in pressure coefficients over the chordwise extents of porous area varied in the same manner, the differences being of the order of 4.25 for 8 percent, 1.95 for 2 percent, and 0.80 for 1 percent.

A porous material having less over-all porosity would reduce the local circulation and hence the initial drop in lift coefficient with the blower off, but with the blower operating, larger power requirements would be needed.

After noting the initial drops in lift coefficient obtained on previous configurations, configuration (f) (last 1 percent) was tried in an effort to reduce the initial drop while maintaining some of the additional lift due to suction. Figure 10 shows that the maximum change in pressure coefficient for this configuration would be of the order of 0.18 as compared with 0.80 for configuration (c) (first 1 percent). Figure 9(e) shows that the initial drop in lift coefficient was less for configuration (f), as was expected, but that no subsequent gain in lift coefficient with suction was obtained.

Another point worth noting is that a larger initial drop in lift coefficient occurred with airplane engine power on than with airplane engine power off and, generally, a higher value of flow coefficient was required to regain this initial lift loss with airplane engine power on.

A comparison of the various data presented in figure 9 indicates that none of the leading-edge configurations tested was clearly superior with regard to increasing the maximum lift coefficient. Although the increment in lift coefficient for a given increment in flow coefficient was greater for some configurations, the initial drop in lift coefficient was generally larger for those same configurations so that the maximum lift coefficient with the maximum suction available remained much the same for most of the configurations tested. Had these same extents of porous area been tested on a sharp-nosed airfoil where leading-edge separation is more likely to occur than with the relatively blunt leading edge of the NACA 2412 airfoil (see fig. 1(d)), the results would undoubtedly have been much more favorable.

It will be noted that there are three parts of figure 9 labeled "full 8 percent." The data of figure 9(a) were obtained just after the installation of the additional leading-edge stiffeners and those of figure 9(g) were obtained during a flight in rain made 184 days total time, 18 hours 9 minutes flight time, after that for figure 9(a). The data of figure 9(h) were obtained 2 days after the rain flight for comparison with the rain flight. Because the intensity of the rain varied from a drizzle to rather heavy rain during the rain flight, not very much can be gained from such a comparison. One point which appears worthy of comparison, however, is in connection with the initial drop in lift coefficient. This initial drop is less for the rain data (fig. 9(g)) than for the dry-air data (fig. 9(h) or 9(a)). This difference is to be expected inasmuch as the rain tends to increase the over-all density of the porous material and thus reduces the local circulation through it.

Figures 9(a) and 9(h) provide a better comparison since the conditions were more similar. A total time of 186 days, a flight time of 19 hours 46 minutes, occurred between the flights from which these data were obtained. The only major difference between these data is the greater initial drop in lift coefficient for the data of figure 9(h). This difference is probably a consequence of the higher porosity which existed for the last tests made (see tests 8 and 9, fig. 5).

Early tuft pictures showed that the stall originated at the trailing edge of the center section with power off and just inboard of the ailerons with power on. Configuration (e) (center section only) and configuration (g) (outboard sealed) were tested in an attempt to influence the origin of the stall but, as is discussed subsequently, the tests were unsuccessful. In obtaining data with configuration (d) (fig. 9(d)), a severe vibration of the leading edge on the outer panels occurred which, for the maximum blower condition, could be seen with the aid of a mirror and could be heard over the noise of the airplane engine and the boundary-layer-control engine and blower. The resulting pressure records were such that no values of flow coefficient could be obtained for the maximum-blower condition and, therefore, estimated values of flow coefficients were used for this condition. The vibration of the leading edge was so violent that the pilot and engineer-observer deemed it advisable to terminate the maximum-blower tests before completion. The pressure records indicate that the vibration continued down through the blower speed range but with much reduced violence so that it could no longer be seen or heard and the pressure records became readable. Apparently, the sealed outer ducts acted as closed organ pipes and reinforced the pressure pulses originating at the blower. The vibration of the leading edge may have been at least partly responsible for the loss of lift with increased suction shown in figure 9(d).

The data for configuration (g) (outboard sealed) shown in figure 9(f) are very similar to data for the original full-8-percent configuration

of figure 9(a) except that the initial drop in lift coefficient is slightly less and the lift coefficients at maximum blower speed are slightly greater.

Comparison of flight and wind-tunnel results.- A comparison of some results from the flight-test investigation with those from unpublished two-dimensional wind-tunnel data obtained before beginning the flight investigation is shown in figure 11. The wind-tunnel model was a 36-inch-chord model of the NACA 2412 airfoil section with a porous nose consisting of filter cloth, similar to that used on the airplane, backed with sintered bronze for stiffness. Wind-tunnel data were obtained at a speed of 78.5 mph. For the particular results shown, the nose of the wind-tunnel model was sealed from the leading edge to the 0.4-percent-chord station and was open for the next 7.3 percent. This wind-tunnel configuration was the one nearest the 8-percent-open configuration used on the airplane. The flight data used were obtained with airplane engine power off and flaps up. A comparison of leading-edge porosities applicable to the flight and wind-tunnel results is shown in figure 11(a). The curve for the wind-tunnel results represents only a small portion of the velocity and differential pressure range tested. The two sets of data are considered to be in good enough agreement for a reasonable comparison of aerodynamic results. Figure 11(b) shows the variation of maximum lift coefficient with flow coefficient to be of the same order of magnitude for the two sets of data. The intercept of the wind-tunnel curve with zero suction was not available but the trend indicated by the dashed line was estimated from other results from the same investigation. The wind-tunnel data show a net gain in lift coefficient (from the sealed case) of only 0.25 at the optimum value of  $C_Q = 0.002$ . An interesting observation is that almost the same increment in lift coefficient was obtained in flight with the maximum available flow coefficient, although the trend indicates that a larger increment in lift coefficient would have been obtained had higher flow coefficients been available.

Tuft pictures.- Figure 12 shows a typical frame from tuft photographs. This frame was taken during the flight with the leading-edge configuration (b) (first 2 percent) in a semistalled condition, with power off, and with flaps down at the maximum-suction condition. As mentioned previously, the tuft pictures were taken by a camera mounted above and behind the wing, facing rearward and upward, and shooting into a spherical mirror. Although the use of the spherical mirror resulted in appreciable distortion, it was used because it permitted an image of the entire wing to be obtained with a single camera. The chordwise strips on the wing were 27.25 inches apart (approximately 12.5 percent of the semispan).

Stall patterns were similar for a given power configuration regardless of leading-edge configuration, amount of suction, or flap position. In general, the stall originated at the right side of the center-section

trailing edge with power off and at the trailing edge just inboard of the ailerons with power on. The stalled areas spread forward and spanwise in a triangular fashion. Such differences in stall pattern as were observed could not be definitely correlated with flap position, leading-edge configuration, or amount of suction.

#### CONCLUDING REMARKS

Results of this investigation have indicated that a practical wing having porous-leading-edge suction can be constructed which has sufficient strength and durability for use in flight without adding excessive weight. For the type of porous material used in this investigation, clogging due to atmospheric dust did not appear to be a problem. For the light rain encountered in flight, the power required to produce a given flow coefficient was about 50 percent more than that required for the dry condition. Based on the ground data, it was estimated that for flight in heavy rain the power would be approximately twice that for the dry condition. At maximum blower speed, however, the porous area became cleared within 3 to 4 minutes after water ceased to impinge on the surface. Under certain conditions, tests showed a severe vibration of the porous material induced by an "organ pipe" resonance of the air column within the ducts. As expected from previous wind-tunnel results, the use of leading-edge suction with the small amount of power available and with the well-rounded airfoil section used (NACA 2412) had little effect on the maximum lift coefficient developed. In general, an appreciable drop in maximum lift coefficient occurred from the leading-edge-sealed configuration to the condition of zero suction with the porous-area configurations tested. Increments in lift coefficient due to the suction available generally brought the maximum lift coefficient back approximately to the value for the wing with the leading edge sealed. The maximum theoretical aerodynamic power, if duct losses are excluded, varied with the configurations tested from 3.65 to 9.70 horsepower.

Langley Aeronautical Laboratory,  
National Advisory Committee for Aeronautics,  
Langley Field, Va., October 26, 1953.

## APPENDIX

## ESTIMATION OF LEADING-EDGE SURFACE PRESSURE

Since no wing surface orifices were provided, the division of the theoretical aerodynamic suction power required (called useful power herein for simplicity) into power required to overcome porous-material drag and power required to reduce duct pressure to average surface pressure was calculated in the following manner: The pressure in the duct  $p_1$  for blower idling and with exit-duct shutter valves closed is assumed to be equal to the average pressure over the porous area  $p$  at the same value of lift coefficient with the blower at maximum speed. In order to determine the average pressure over the porous area at some higher value of lift coefficient with blower operating, this pressure is expressed in terms of pressure coefficient  $S$  by means of the equation  $S = (H_0 - p)/q_c$  where  $H_0$  and  $q_c$  are free-stream total and calibrated impact pressures, respectively. The pressure coefficient is corrected to the proper value of lift coefficient by the method described below and the new surface pressure may then be calculated.

The process of correcting for lift coefficient consisted of calculating theoretical pressure coefficients for the wing upper surface at various values of lift coefficient obtained from data in reference 5, integrating and determining the average pressure coefficient over the first 8 percent, and plotting these average pressure coefficients against lift coefficient. The pressure coefficient determined from flight data without suction is located on this plot at its corresponding lift coefficient and a curve parallel to the calculated theoretical curve is passed through the test point. The pressure coefficient at the lift coefficient for maximum blower speed can then be picked from this new curve. With the surface pressure  $p$  thus determined, the pressure difference across the porous material is

$$\Delta p = p - p_1$$

and the initial pressure to be overcome by the blower is

$$H_0 - p = S q_c$$

These equations are based on the assumption that the dynamic pressure does not assist the flow to pass through the porous material.



## REFERENCES

1. Jones, Melvill, and Head, M. R.: The Reduction of Drag by Distributed Suction. Third Anglo-American Aeronautical Conference (Brighton), Sept. 4-7, 1951, pp. 199-230.
2. Raspet, August: Boundary Layer Studies on a Sailplane. Preprint No. 348, S.M.F. Fund Preprint, Inst. Aero. Sci., Jan.-Feb. 1952.
3. Miles, F. G.: Sucking Away the Boundary Layer. Flight, vol. XXXV, no. 1570, Jan. 26, 1939, pp. 82b-82d.
4. Henry, John R.: Design of Power-Plant Installations. Pressure-Loss Characteristics of Duct Components. NACA WR L-208, 1944. (Formerly NACA ARR L4F26.)
5. Abbott, Ira H., Von Doenhoff, Albert E., and Stivers, Louis S., Jr.: Summary of Airfoil Data. NACA Rep. 824, 1945. (Supersedes NACA WR L-560.)

TABLE I.- DIMENSIONAL DATA FOR TEST AIRPLANE

|  |           |
|--|-----------|
| <sup>a</sup> Approximate take-off weight, lb . . . . .                   | 3,830     |
| Horsepower (at 2,200 rpm) . . . . .                                      | 240       |
| Propeller diameter, ft . . . . .   | 7.75      |
| Over-all length, ft . . . . .  | 27.10     |
| Wing:  |           |
| Area (including fuselage), sq ft . . . . .                               | 218.13    |
| Span, ft . . . . .   | 36.17     |
| Dihedral, deg . . . . .  | 0.7       |
| Aspect ratio . . . . .   | 6.00      |
| Taper ratio . . . . .  | 0.62      |
| Mean aerodynamic chord, ft . . . . .                                     | 6.30      |
| Incidence, deg . . . . .   | 1.0       |
| Washout, deg . . . . .   | 1.5       |
| Airfoil section . . . . .  | NACA 2412 |
| Flap area, sq ft . . . . .   | 8.68      |
| Aileron area, sq ft . . . . .  | 12.32     |
| Flap deflection, down, deg . . . . .                                     | 45        |
| Aileron deflection, deg . . . . .  | ±25       |
| Horizontal tail:   |           |
| Aspect ratio . . . . .   | 3.16      |
| Total area, sq ft . . . . .  | 35.20     |
| Stabilizer area, sq ft . . . . .   | 19.79     |
| Elevator area (less tab), sq ft . . . . .                                | 14.66     |
| Elevator tab area, sq ft . . . . .                                       | 0.75      |
| Airfoil section . . . . .  | NACA 0006 |
| Tail length (center of gravity to elevator hinge, approx.), ft . . . . . | 18.0      |
| Elevator deflection, deg:  |           |
| Up . . . . .   | 31.5      |
| Down . . . . .   | 13.5      |
| Elevator tab deflection, deg:  |           |
| Up . . . . .   | 12        |
| Down . . . . .   | 31        |
| Incidence, deg . . . . .   | -4        |
| Vertical tail:   |           |
| Aspect ratio . . . . .   | 0.88      |
| Total area, sq ft . . . . .  | 16.55     |
| Fin area, sq ft . . . . .  | 8.78      |
| Rudder area, sq ft . . . . .   | 7.77      |
| Airfoil section . . . . .  | NACA 0006 |
| Rudder deflection, deg . . . . .   | ±21       |
| Tail length (center of gravity to rudder hinge, approx.), ft . . . . .   | 18.3      |
| Fin offset, deg . . . . .  | 0         |
| <sup>a</sup> Design gross weight of original airplane, lb . . . . .      | 3,350     |

TABLE II

## COMPONENT WEIGHTS

[All weights in pounds]

|   |        |
|---|--------|
| Porous surfaces:  |        |
| Total . . . . .   | 34.5   |
| Center section . . . . .  | 4.5    |
| Each wing . . . . .   | 15.0   |
| Complete wing with boundary-layer control<br>(including porous surfaces): |        |
| Without fuel . . . . .  | 403.25 |
| <sup>a</sup> With 61 gallons fuel . . . . .                               | 769.25 |
| Complete wing, original airplane:   |        |
| Without fuel . . . . .  | 295.5  |
| With 76 gallons fuel . . . . .  | 751.5  |
| Boundary-layer-control equipment in fuselage . . . . . 458.8              |        |
| Engine . . . . .  | 153.0  |
| Blower . . . . .  | 78.8   |
| Gear box . . . . .  | 42.3   |
| Mount . . . . .   | 47.3   |
| Ducting . . . . .   | 30.0   |
| Accessories (cooling and lubrication, etc.) . . . . .                     | 107.4  |
| Instrumentation . . . . . 455.5   |        |
| Instruments . . . . .   | 163.2  |
| Batteries and inverter . . . . .  | 145.4  |
| Wing booms (including pickup heads) . . . . .                             | 17.5   |
| Camera, mirror, and mounting structure . . . . .                          | 29.3   |
| Mounting boards, cables, relays, tubing, etc. . . . .                     | 99.1   |

<sup>a</sup>The ducting necessitated use of smaller wing fuel tanks.

TABLE III

## POROSITY TESTS

[All porosity tests were run on the ground with the leading-edge configuration listed in figure 4 as configuration (a) (full 8 percent open).]

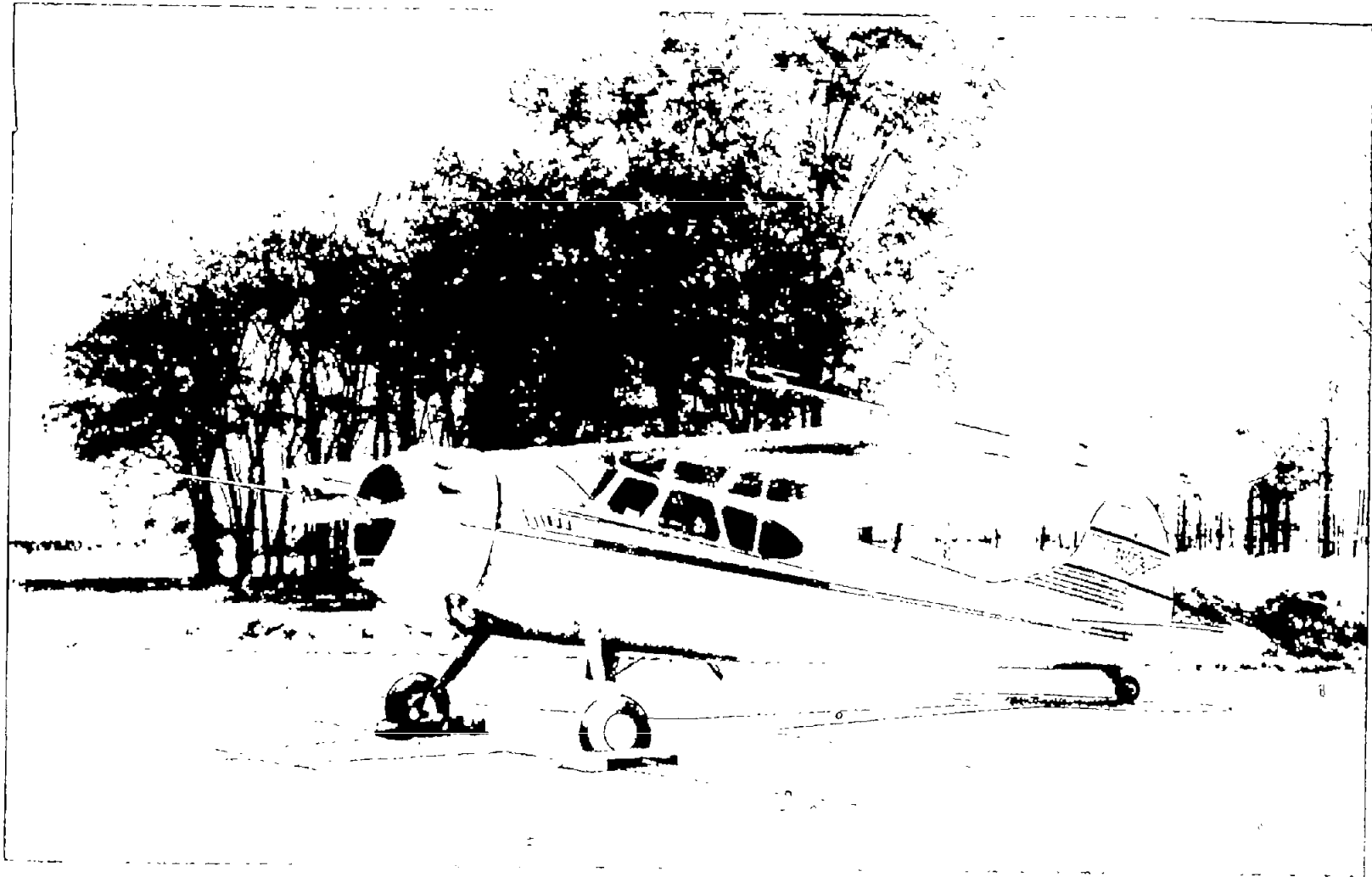
| Test | Flight time since previous test |         | Total time since previous test, days | Remarks   |
|------|---------------------------------|---------|--------------------------------------|---|
|      | Hours                           | Minutes |                                      |   |
| 1    | 0                               |         | 0                                    | Made at beginning of program  |
| 2    | 11                              | 53      | 89                                   | All flights, full 8 percent open  |
| 3    | 13                              | 41      | 113                                  | Division of flight time as follows:<br>7 hr 43 min, full 8 percent open<br>1 hr 02 min, completely sealed<br>2 hr 51 min, first 1 percent open<br>2 hr 05 min, first 2 percent open   |
| 4    | 0                               |         | 0                                    | Removed all tape and cleaned by rubbing surface with lacquer thinner on cloth   |
| 5    | 0                               |         | 0                                    | Sprayed surface with Prep-sol   |
| 6    | 0                               |         | 1                                    | Sprayed surface with benzene  |
| 7    | 0                               |         | 28                                   | Additional stiffeners installed; sprayed carbon tetrachloride through both sides of porous material while removed from wing   |
| 8    | 17                              | 43      | 32                                   | Division of flight time as follows:<br>4 hr 01 min, full 8 percent open<br>2 hr 41 min, first 2 percent open<br>3 hr 39 min, first 1 percent open<br>0 hr 51 min, leading edge sealed<br>1 hr 42 min, center section only open<br>2 hr 21 min, last 1 percent open<br>2 hr 33 min, outboard sealed<br>Limited attempts at cleaning made between flights |
| 9    | 7                               | 00      | 168                                  | Approx. $1\frac{1}{2}$ hr in rain of varying intensity; full 8 percent open   |
|      | 50                              | 17      | 431                                  |   |

TABLE IV  
POWER REQUIREMENTS

| Leading-edge configuration       | Blower (a) | Ratio of useful power to engine output | Ratio of porous-material power to useful power | Ratio of duct power loss to engine output (approx.) | Blower efficiency, percent (approx.) | Engine output, hp | Flow coefficient at stall |
|----------------------------------|------------|--|--|---|--------------------------------------|-------------------|---------------------------|
| Full 8 percent open              | Maximum    | 0.255                                  | 0.332  | 0.0517  | 33.5                                 | 15.8              | 0.00131                   |
|                                  | 2/3        | .217                                   | .282   | .0304   | 27.0                                 | 12.5              | .00098                    |
|                                  | 1/3        | .168                                   | .185   | .0038   | 18.9                                 | 9.1               | .00056                    |
|                                  | Minimum    | .054                                   | .084   | 0   | 6.0                                  | 9.0               | .00020                    |
| First 1 percent open             | Maximum    | .436                                   | .430   | .0302   | 50.7                                 | 17.7              | .00110                    |
| First 2 percent open             | Maximum    | .447                                   | .398   | .0477   | 53.9                                 | 16.8              | .00090                    |
| Last 1 percent open              | Maximum    | .472                                   | .492   | .0125   | 53.0                                 | 20.7              | .00076                    |
| Outboard sealed                  | Maximum    | .272                                   | .360   | .0299   | 32.8                                 | 14.9              | .00114                    |
| Full 8 percent in rain           | Maximum    | .323                                   | .228   | .0326   | 38.9                                 | 14.7              | .00110                    |
| <sup>b</sup> Full 8 percent open | Maximum    | .259                                   | .310   | .0460   | 33.3                                 | 14.1              | .00113                    |

<sup>a</sup>Blower variation is described according to an approximate variation of rotational speed.

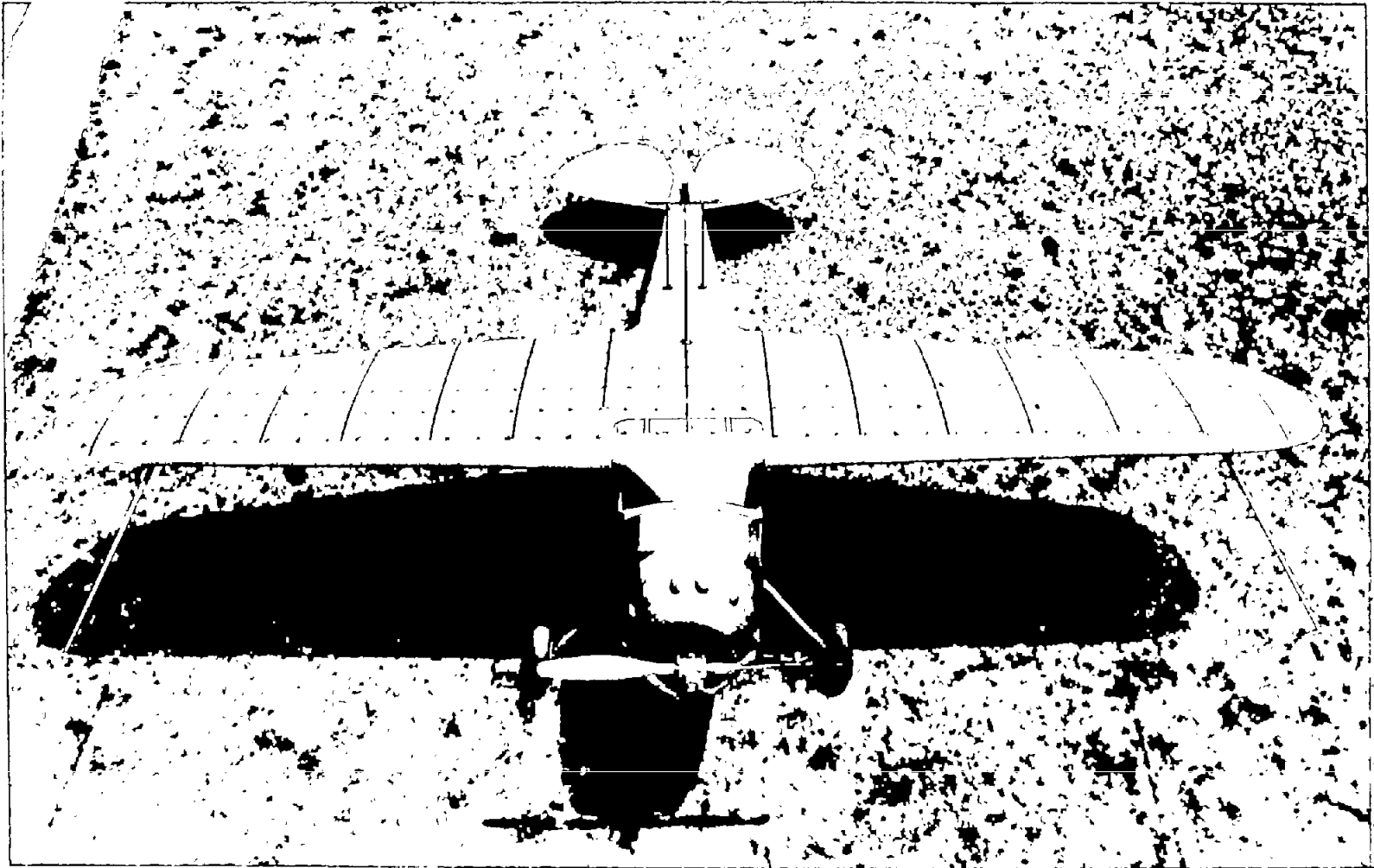
<sup>b</sup>These data were obtained at end of flight program after flight in rain and are presented for comparison with other data obtained early in flight program for same configuration.



(a) One-quarter front view.

L-70267

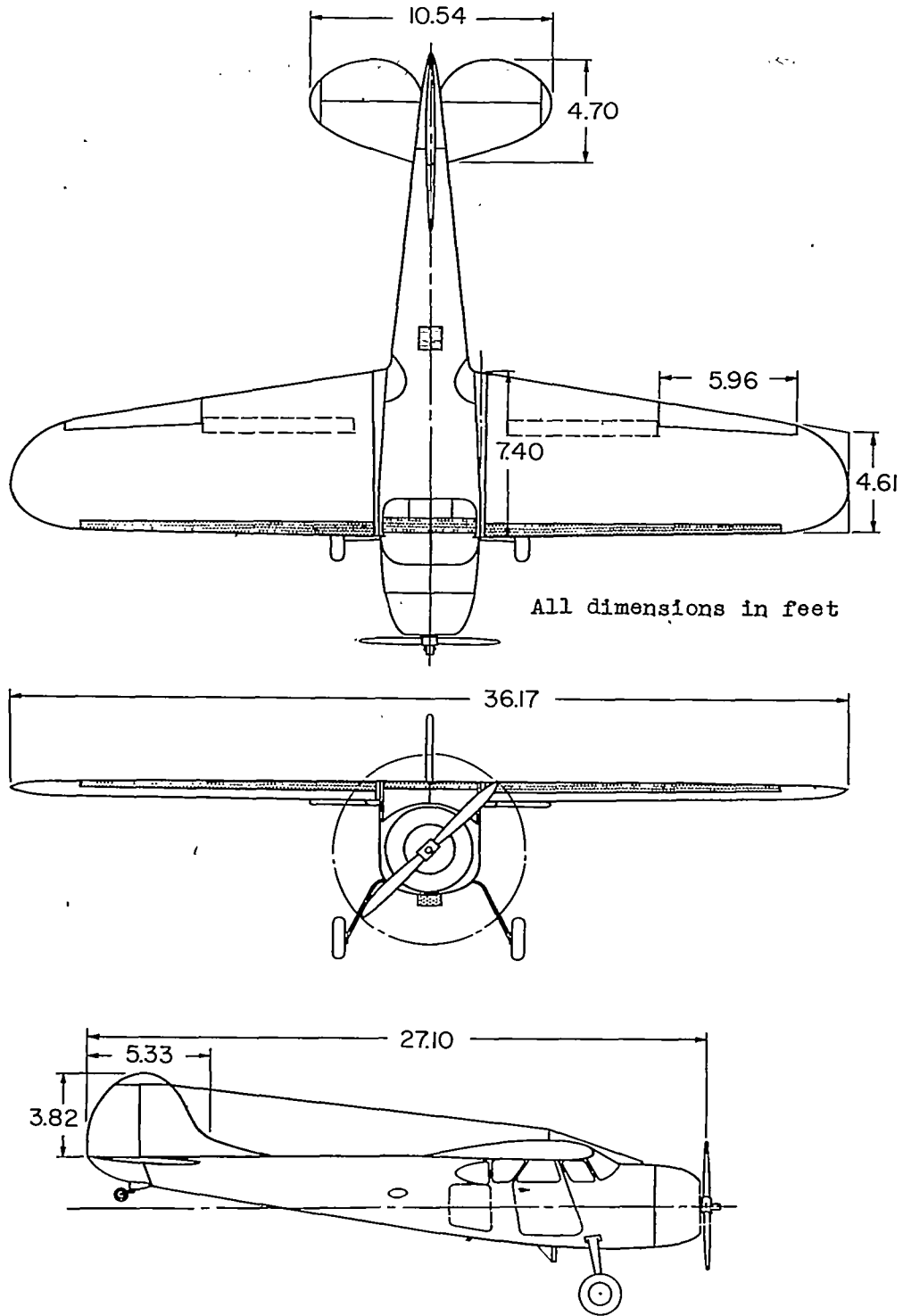
Figure 1.- Cessna 190 airplane used for flight tests.



(b) View from above.

L-71602

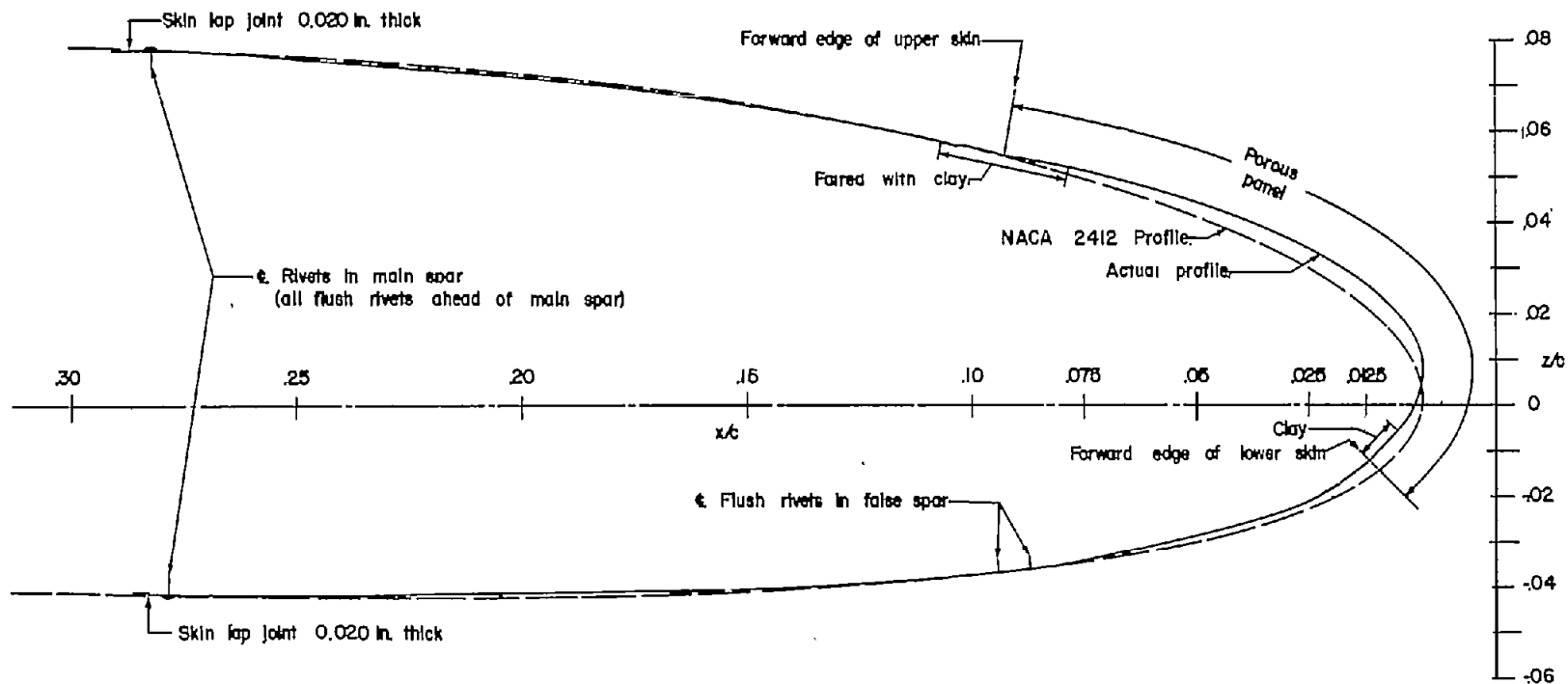
Figure 1.- Continued.



(c) Three-view drawing.

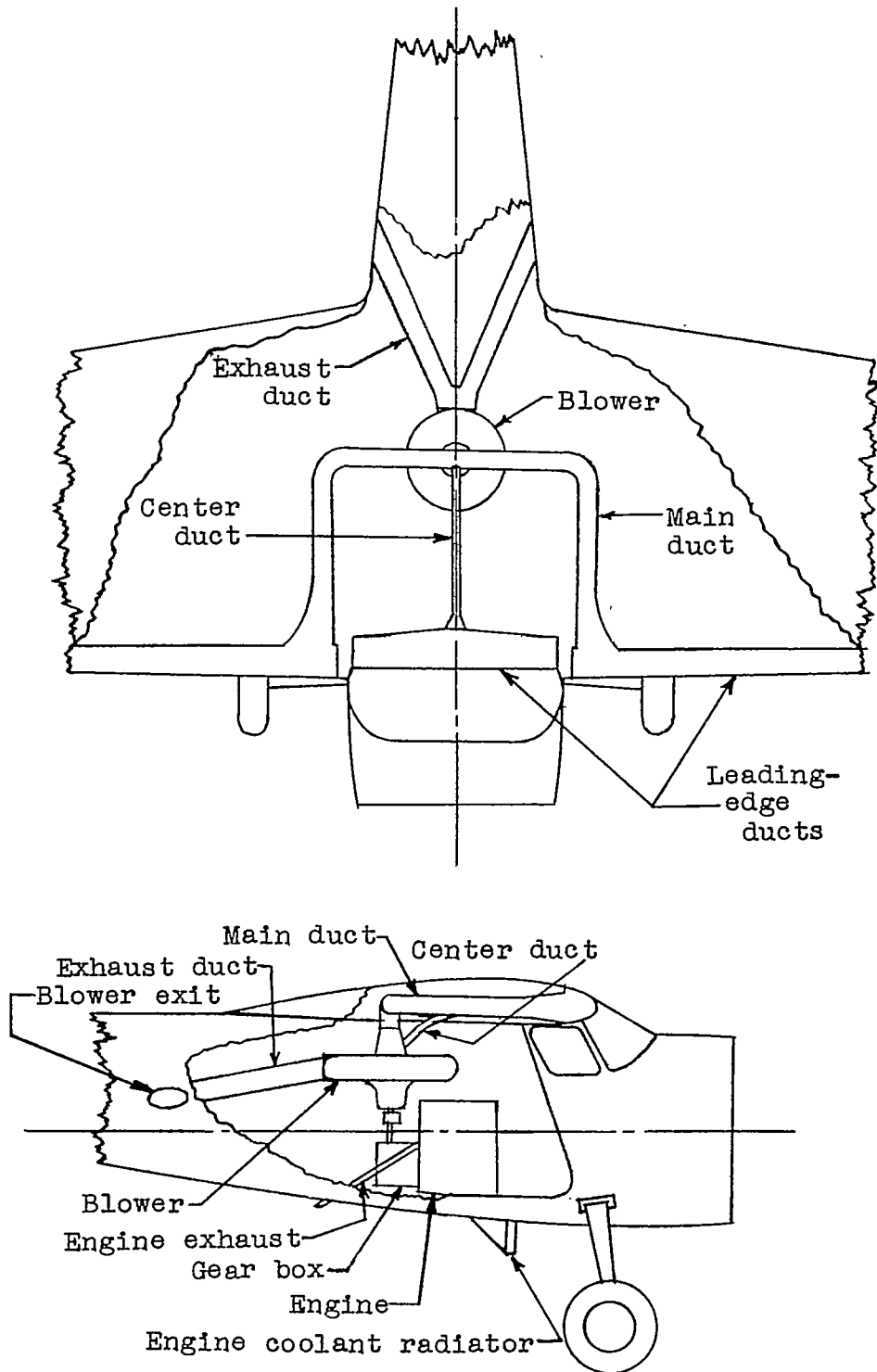
Figure 1.- Continued.





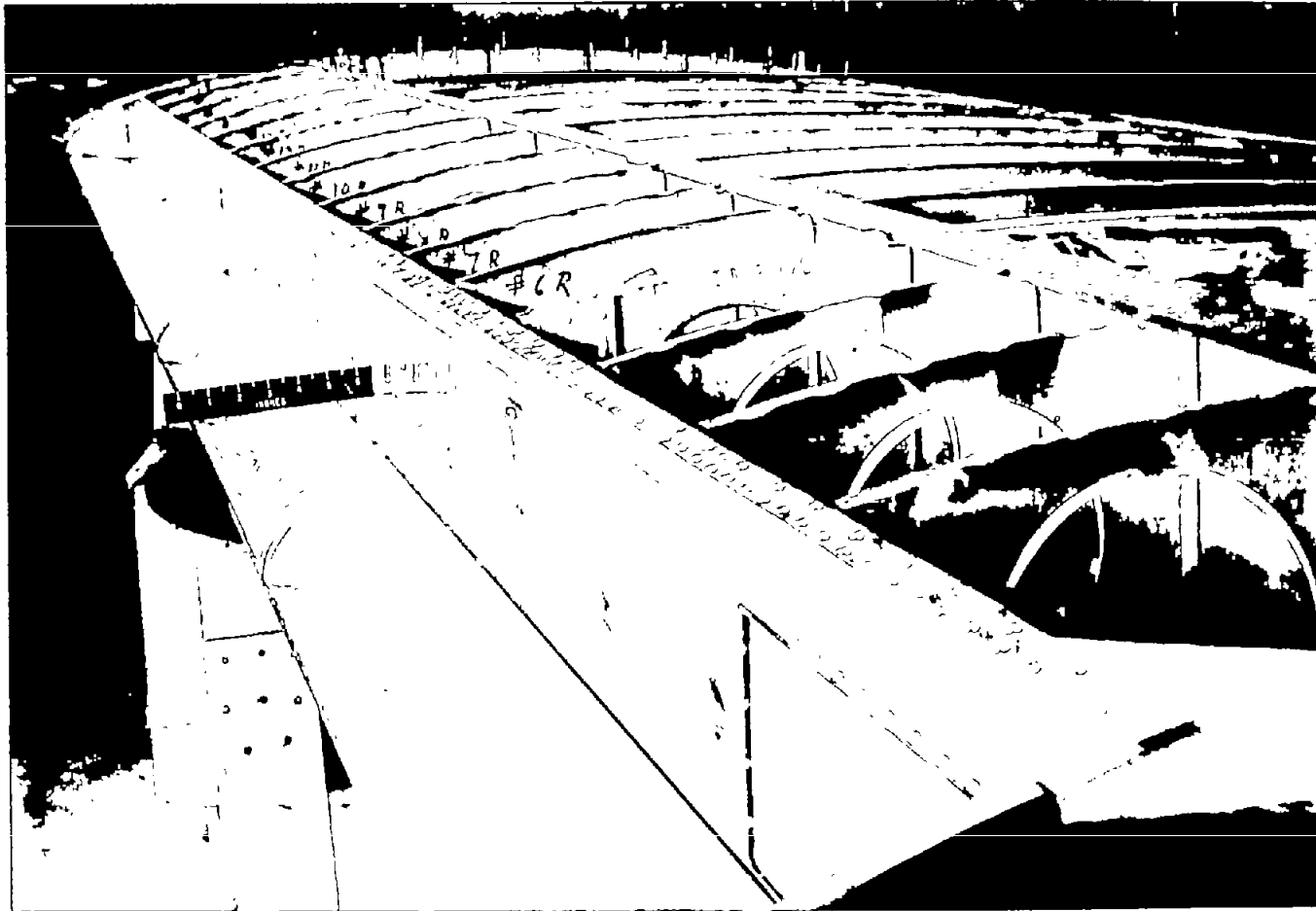
(d) Comparison of actual wing profile with NACA 2412 profile.

Figure 1.- Concluded.



(a) Sketch of equipment installation.

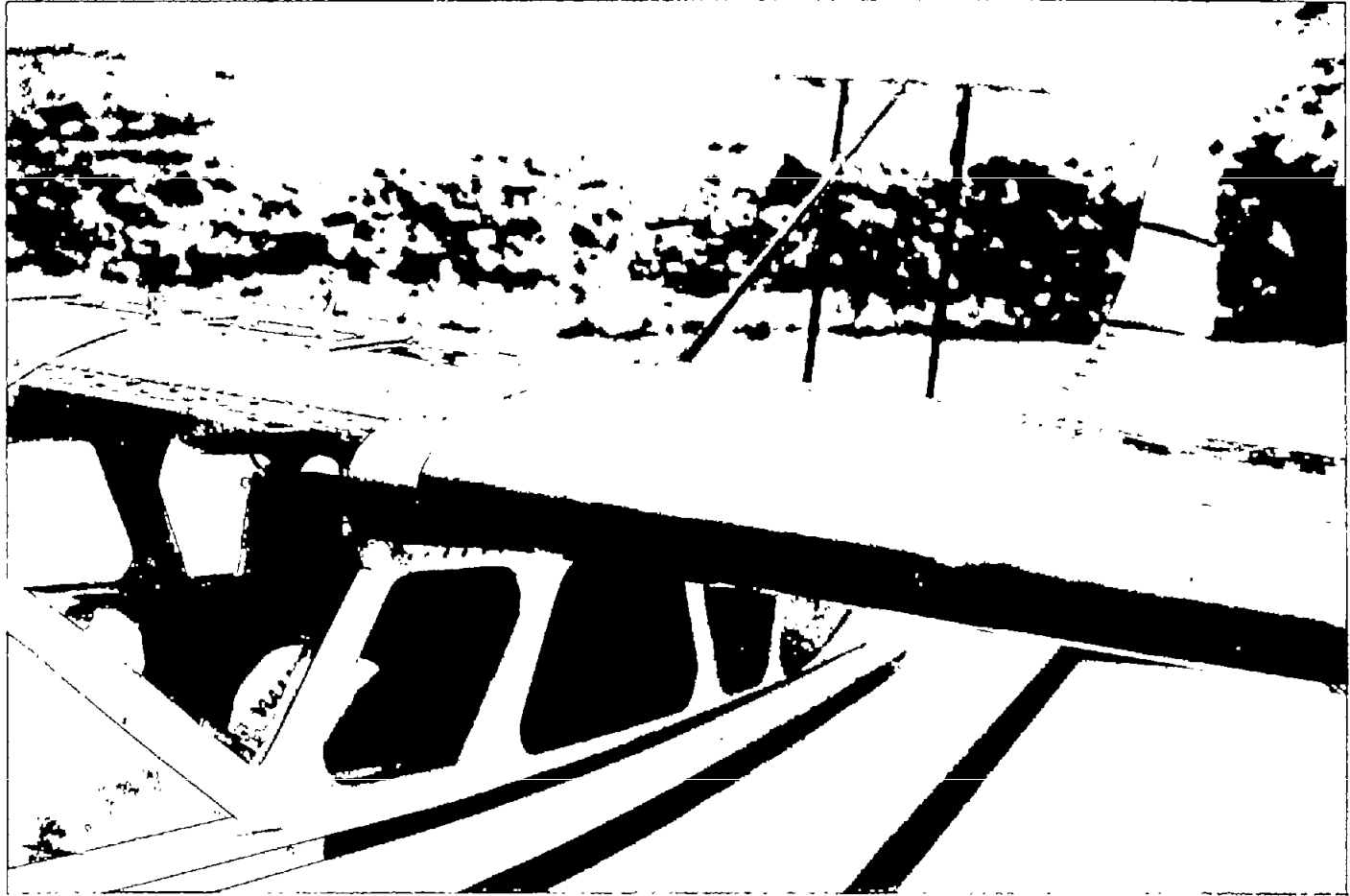
Figure 2.- Equipment installation.



(b) Leading-edge-duct structure.

L-67926

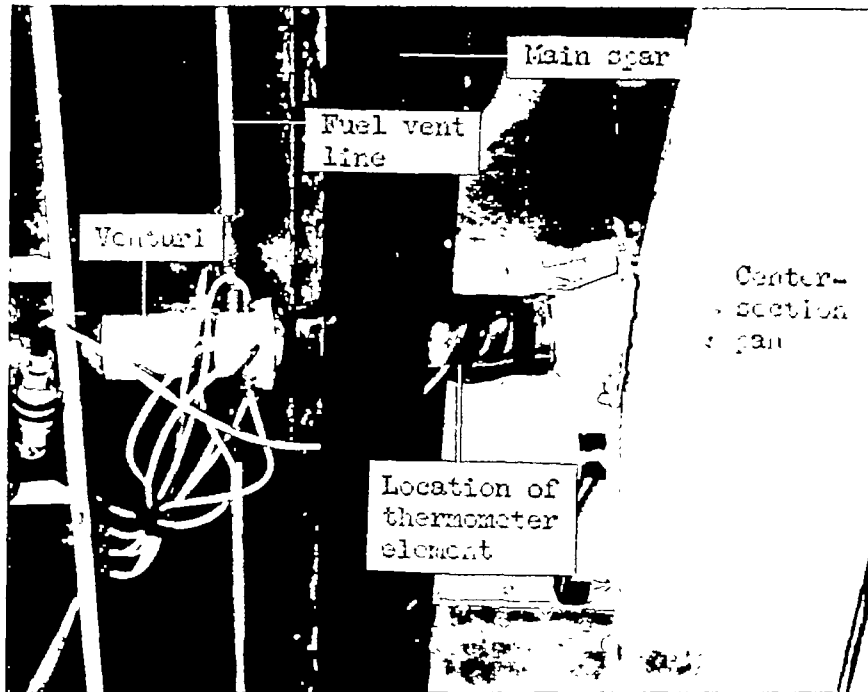
Figure 2.- Continued.



(c) Closeup of porous leading edge.

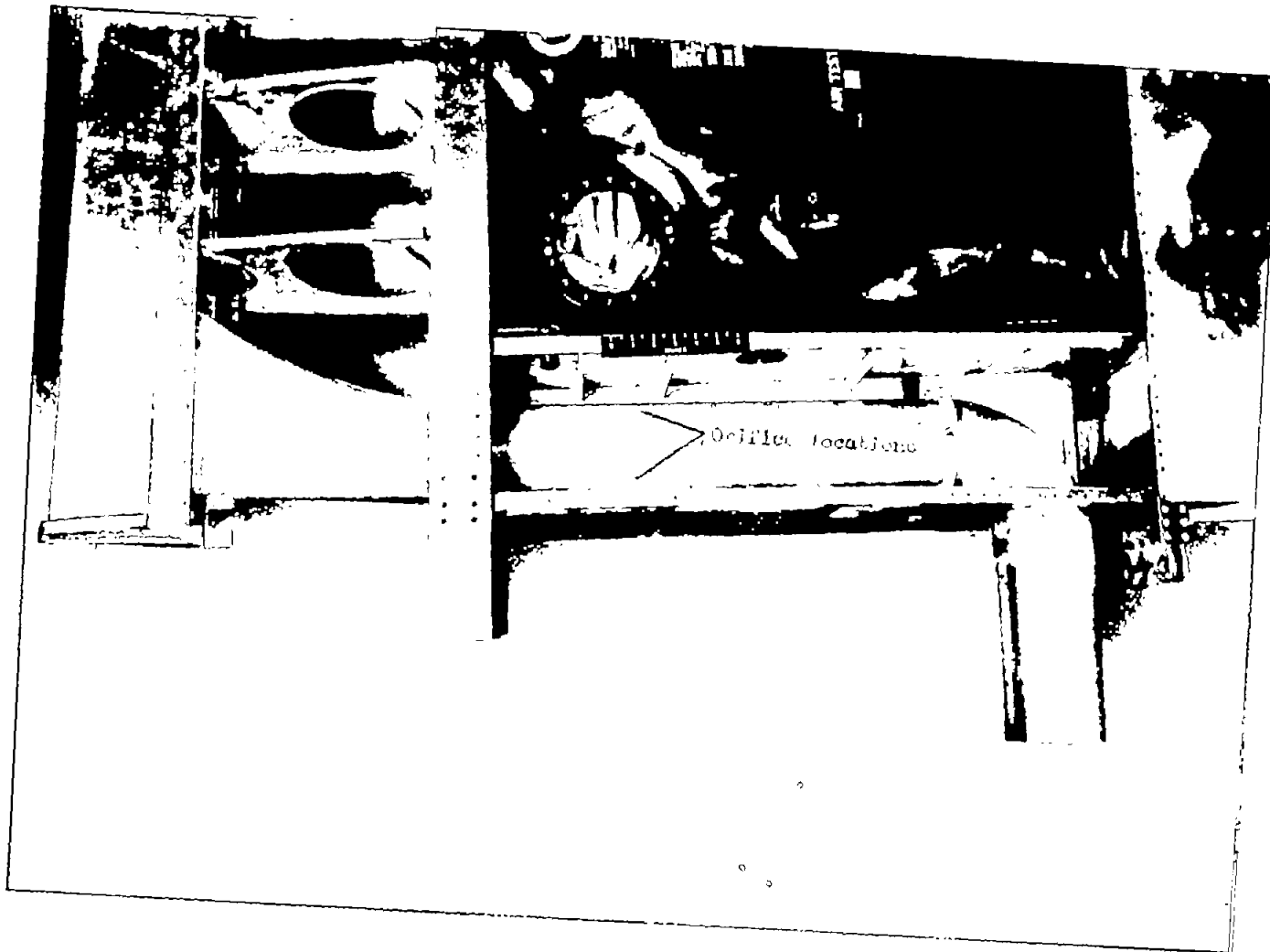
L-70272

Figure 2.- Continued.



(d) Center-duct installation in cabin roof. L-77565.1

Figure 2.- Continued.



(e) Right-main-duct installation. L-67931.1

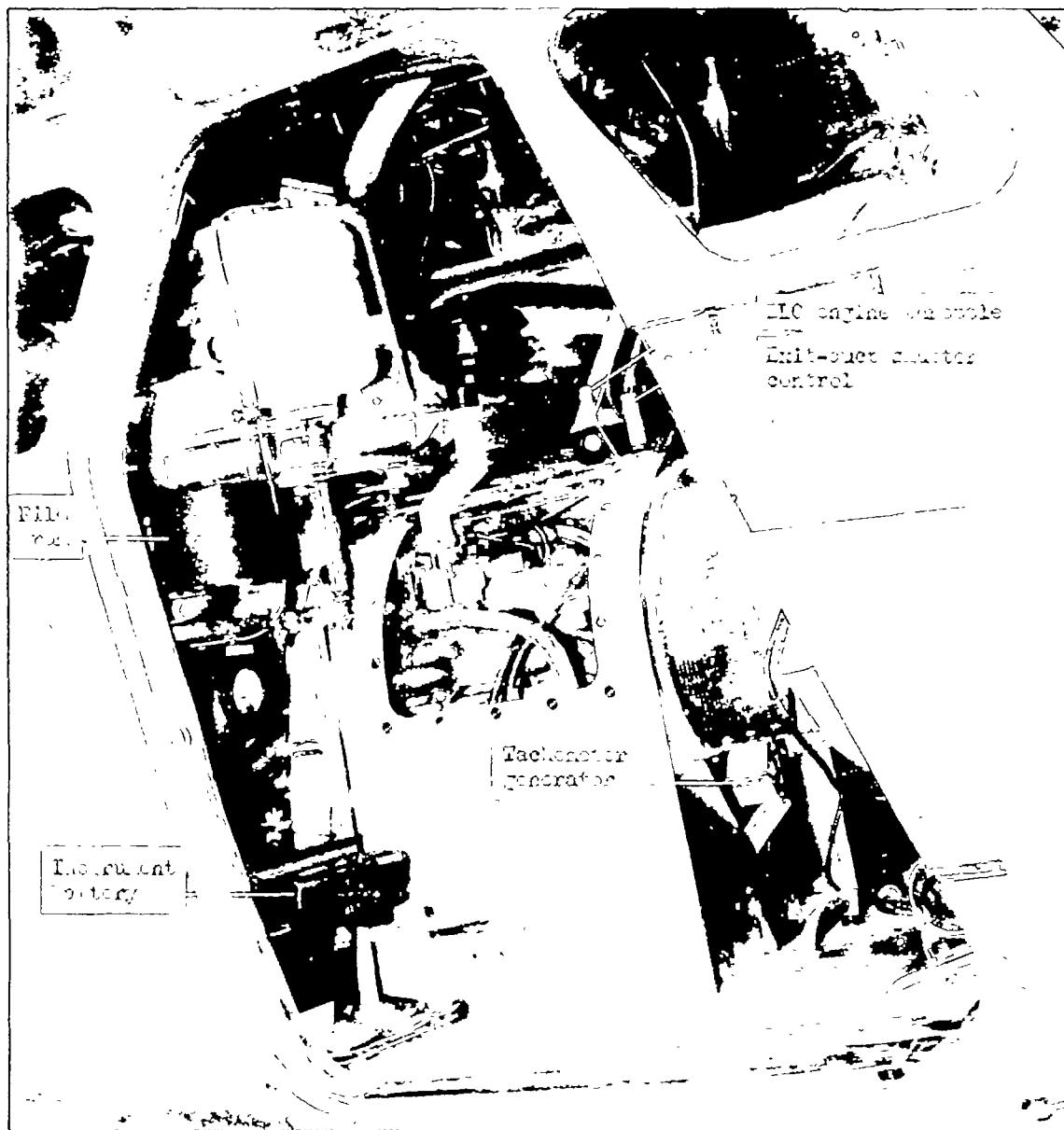
Figure 2.- Continued.



(f) Duct junction and blower.

L-70872.1

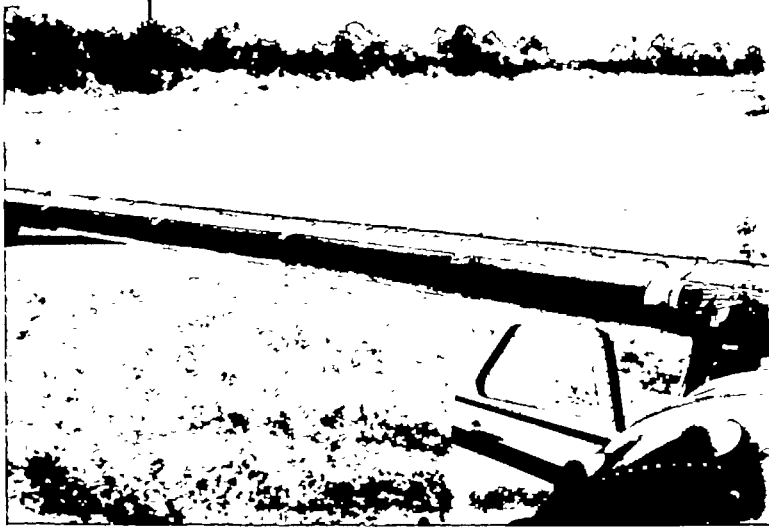
Figure 2.- Continued.



(g) Engine-blower installation. L-70270.1

Figure 2.- Concluded.





(a) Normal.

L-72837



(b) Collapsed.

L-72838

Figure 3.- Effect of suction on unstiffened leading edge with only first 2 percent of leading edge open.

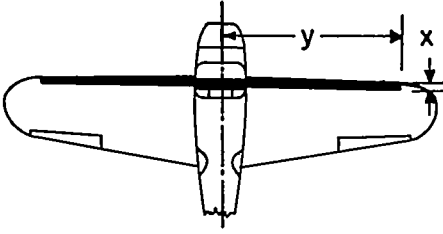
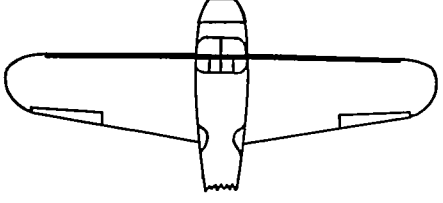
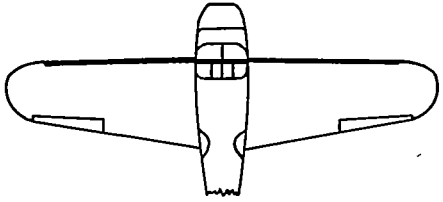
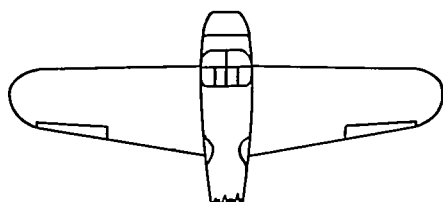
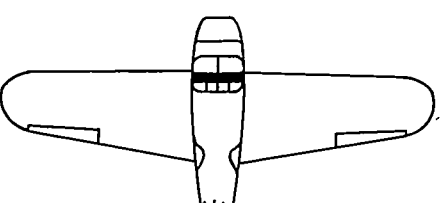
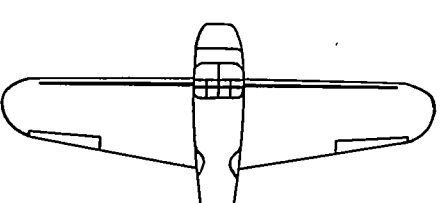
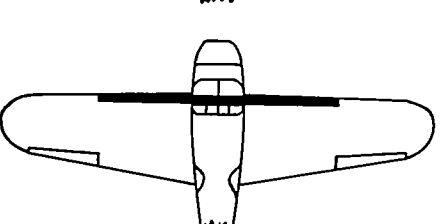
| Configuration   | $x/c$ | $2y/b$ | $S_A'/S_A$ | $S_D/S_A$ |
|---|-------|--------|------------|-----------|
| <br>(a) Full 8 percent open        | 0.08  | 0.834  | 0.892      | 0.081     |
| <br>(b) First 2 percent open       | .02   | .834   | .892       | .029      |
| <br>(c) First 1 percent open       | .01   | .834   | .892       | .018      |
| <br>(d) Sealed                    | 0     | 0      | 0          | 0         |
| <br>(e) Center section only open | .08   | .115   | .145       | .012      |
| <br>(f) Last 1 percent open      | .01   | .834   | .892       | .008      |
| <br>(g) Outboard sealed          | .08   | .548   | .627       | .057      |

Figure 4.- Porous-leading-edge configurations tested.

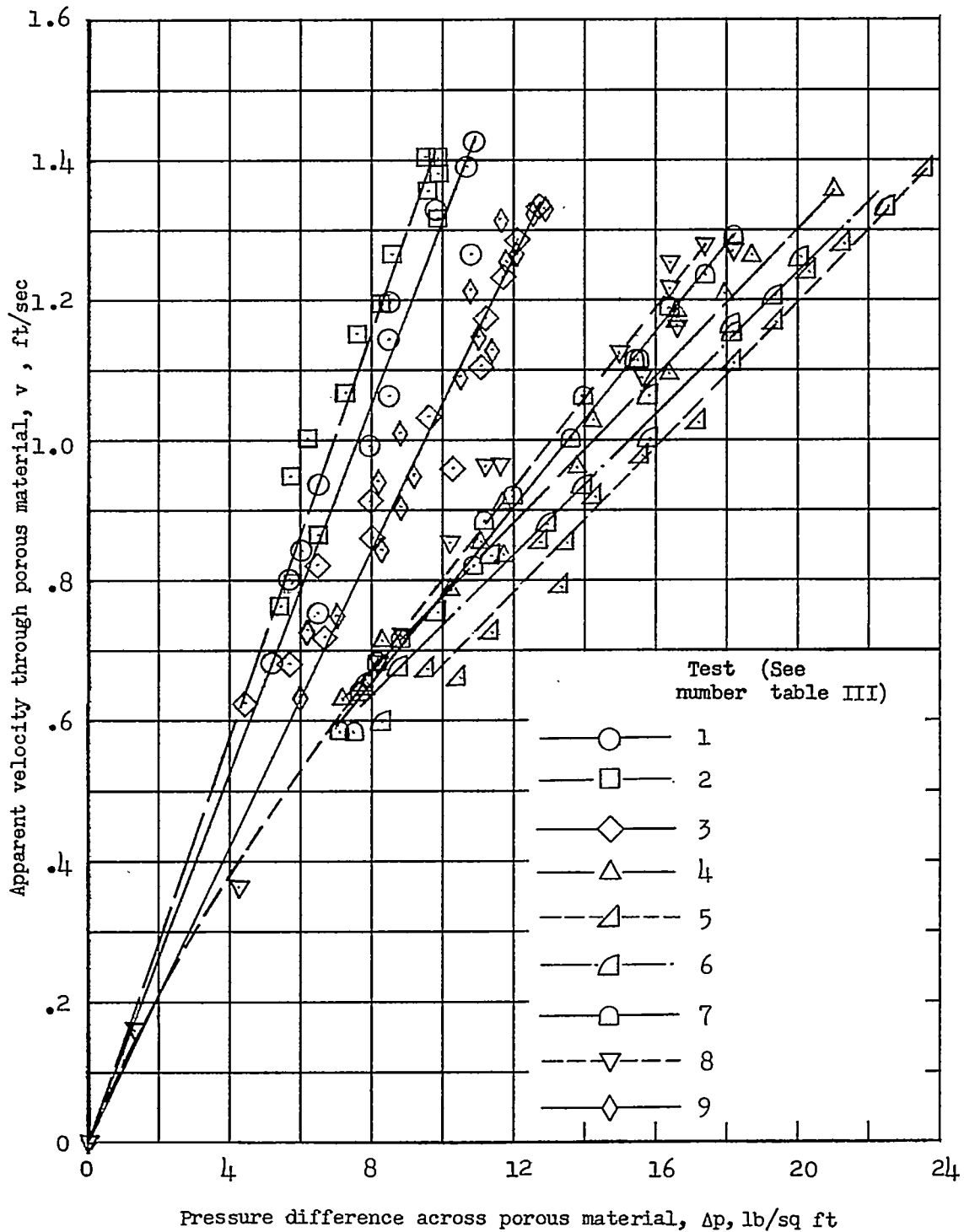


Figure 5.- Variation of apparent velocity through porous material with pressure difference across porous material from ground tests. Leading-edge configuration (a).

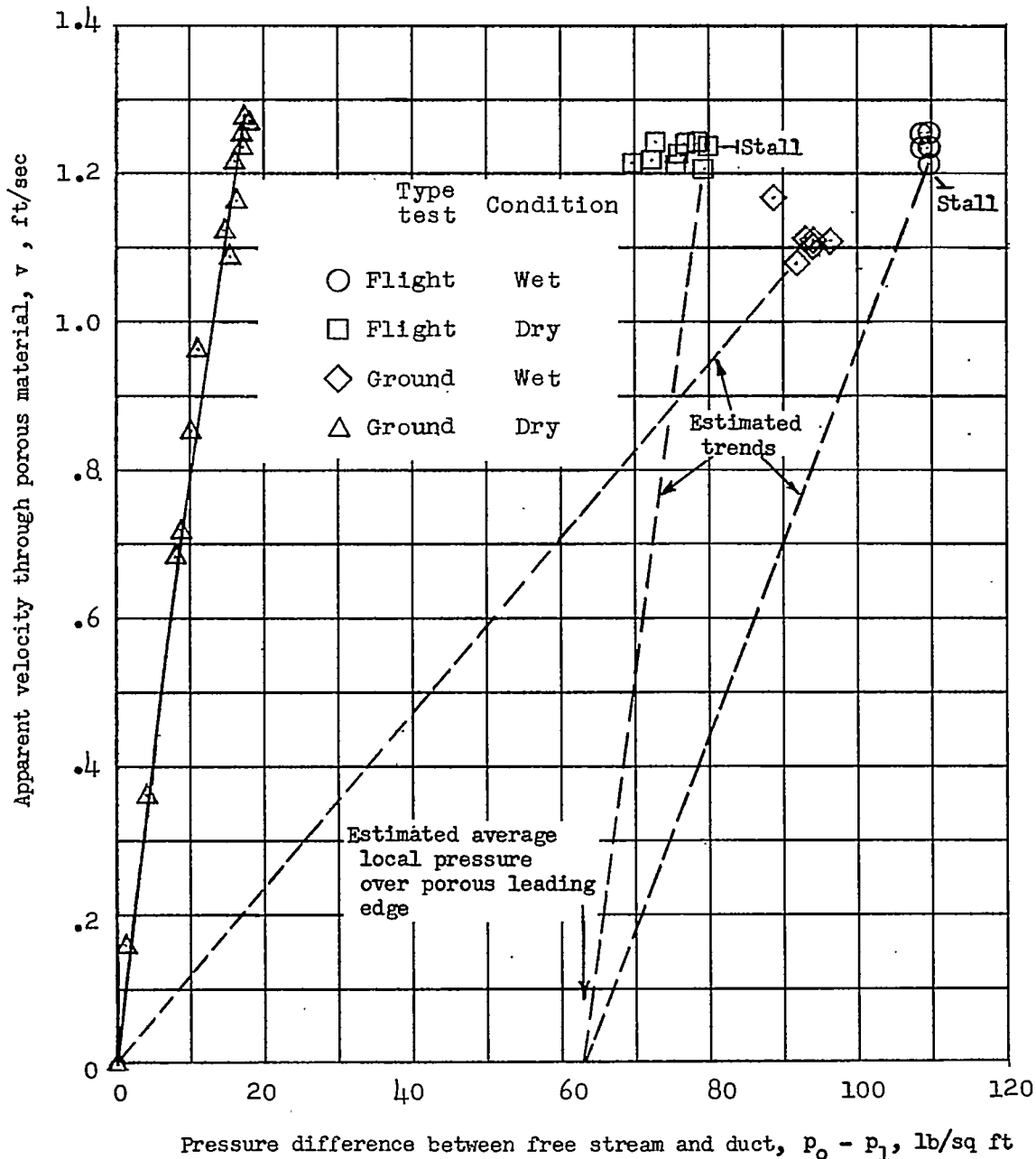


Figure 6.- Effect of rain on porosity of porous leading edge. Leading-edge configuration (a).

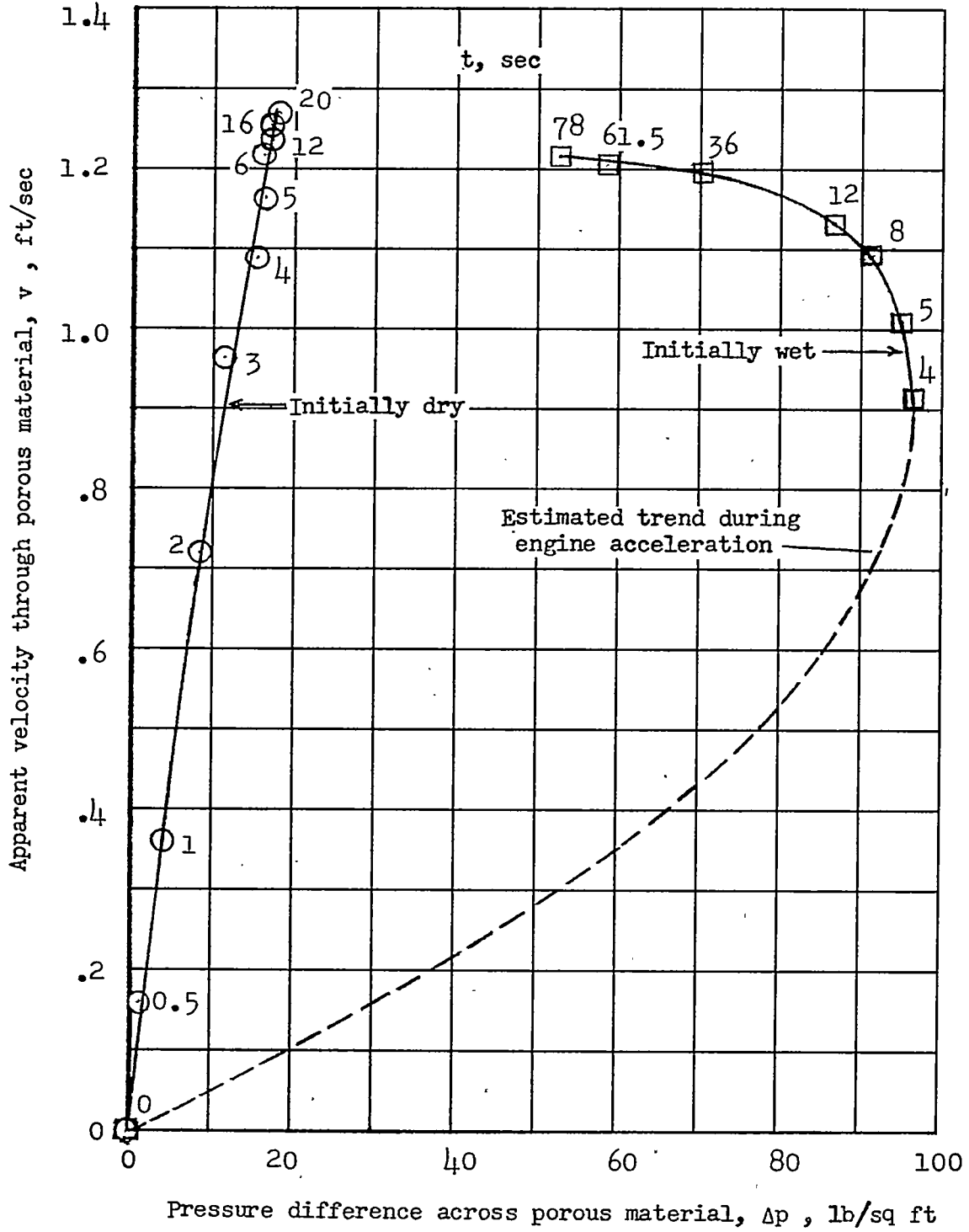


Figure 7.- Variation of apparent velocity through porous material with pressure difference across porous material and time in seconds. Leading-edge configuration (a).

|                                  |                 |
|----------------------------------|-----------------|
| 1. Porous material drag          | 1.34 hp         |
| 2. Power to reduce duct pressure | 2.70 hp         |
| 3. Duct losses                   | .82 hp          |
| 4. Blower losses                 | 9.66 hp         |
| 5. Gearbox losses                | .30 hp          |
| 6. Power for accessories         | 1.00 hp         |
| 7. Total engine output           | <u>15.82 hp</u> |

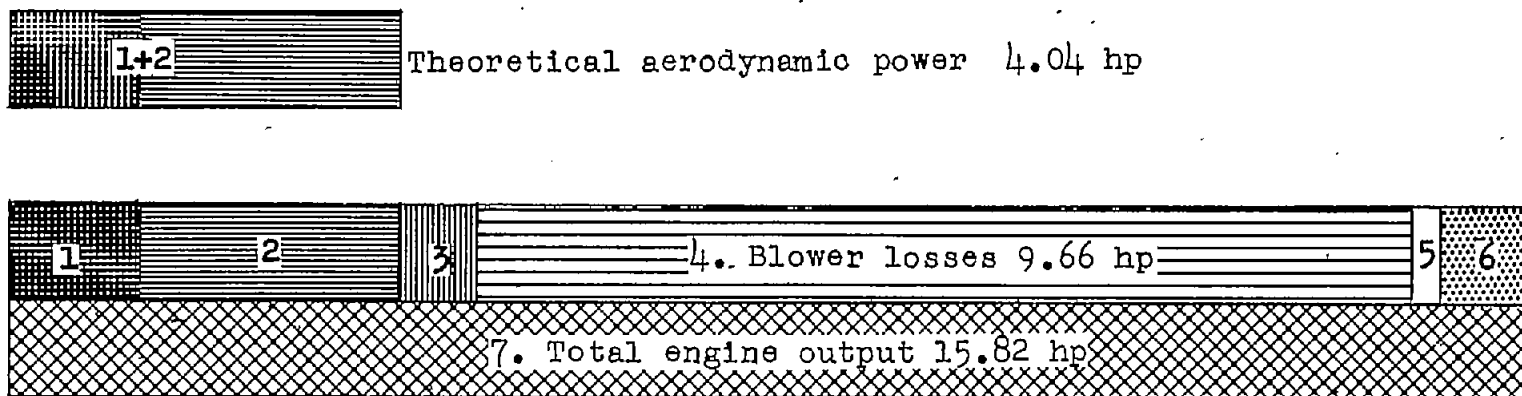


Figure 8.- Estimated distribution of input power for the gliding condition with maximum blower at the stall. Leading-edge configuration (a).

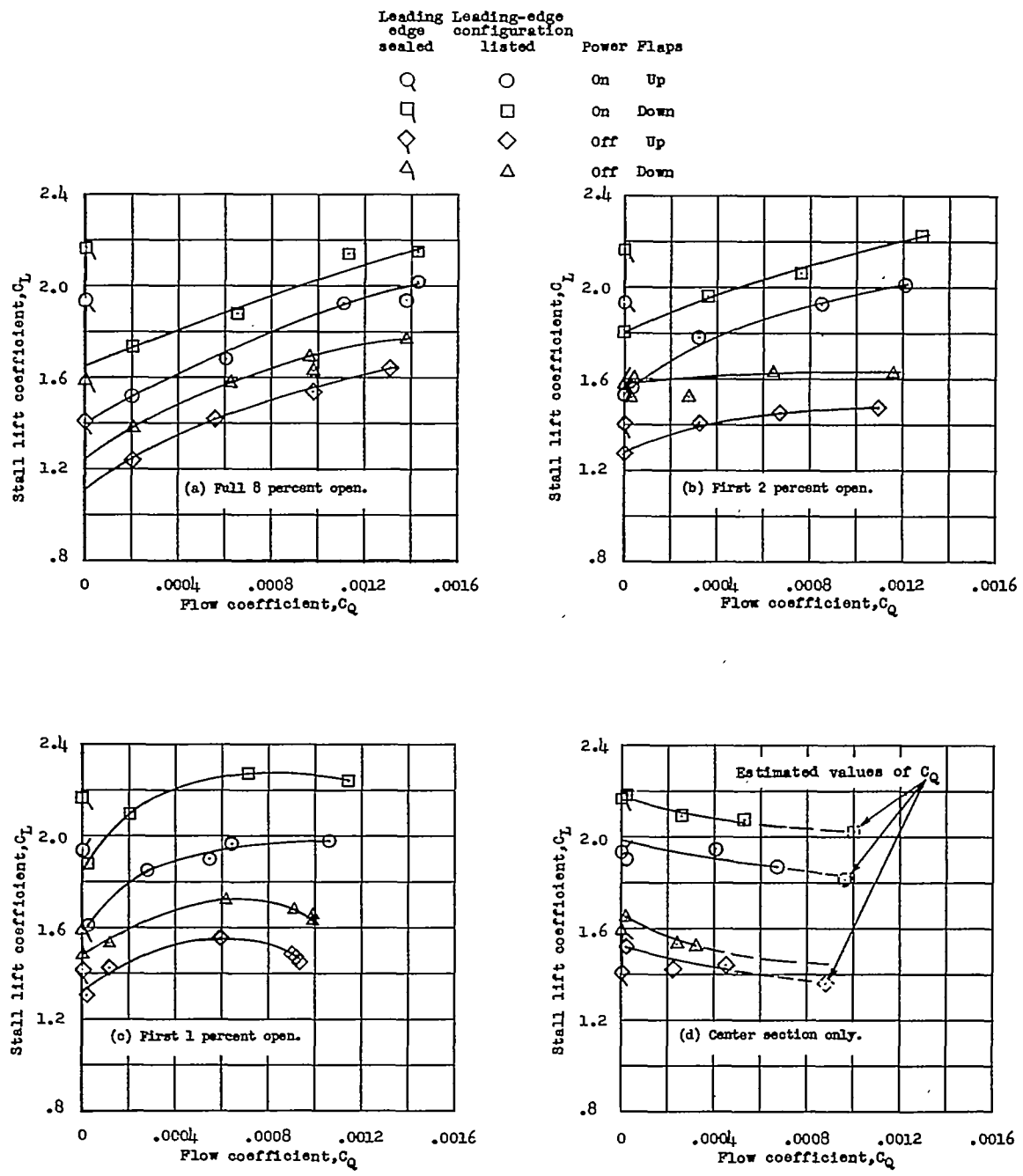


Figure 9.- Variation of lift coefficient at the stall with flow coefficient.

| Leading edge sealed | Leading-edge configuration listed | Power | Flaps |
|---------------------|-----------------------------------|-------|-------|
| ○                   | ○                                 | On    | Up    |
| □                   | □                                 | On    | Down  |
| ◇                   | ◇                                 | Off   | Up    |
| △                   | △                                 | Off   |       |

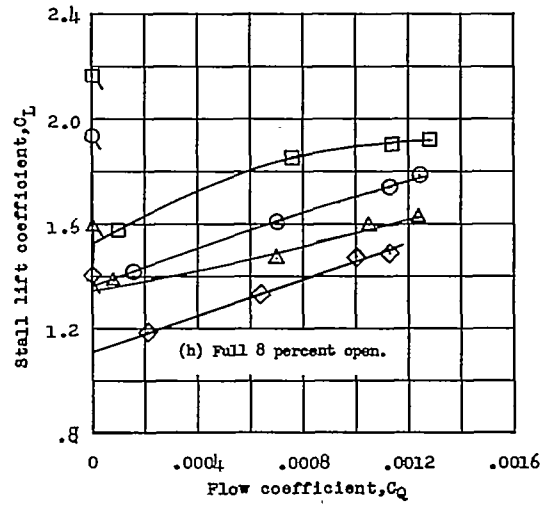
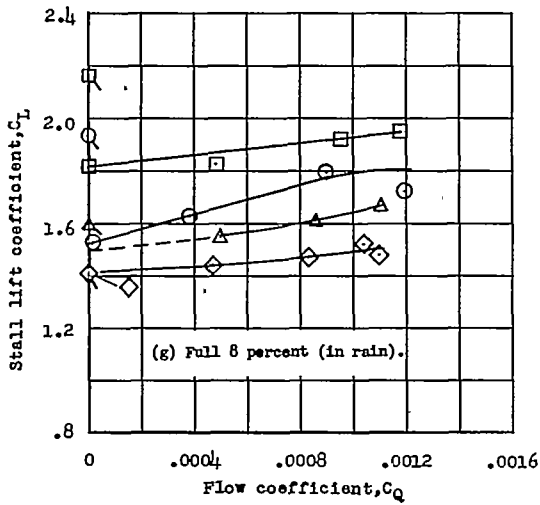
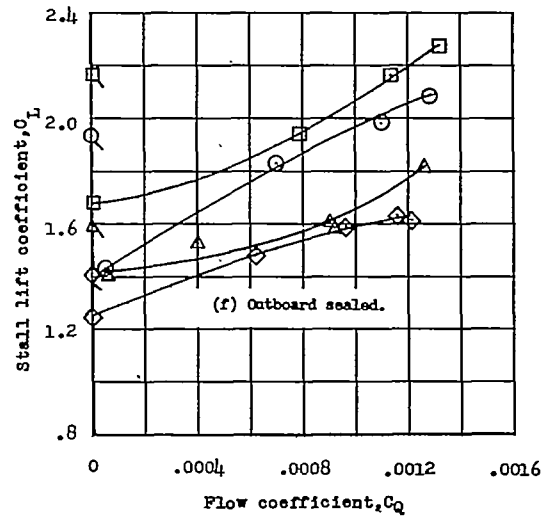
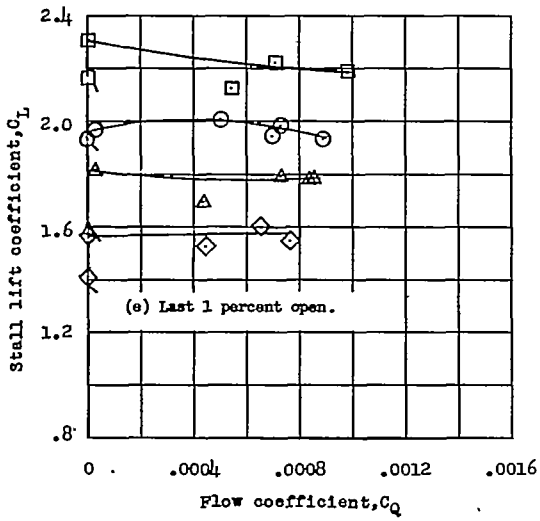


Figure 9.- Concluded.



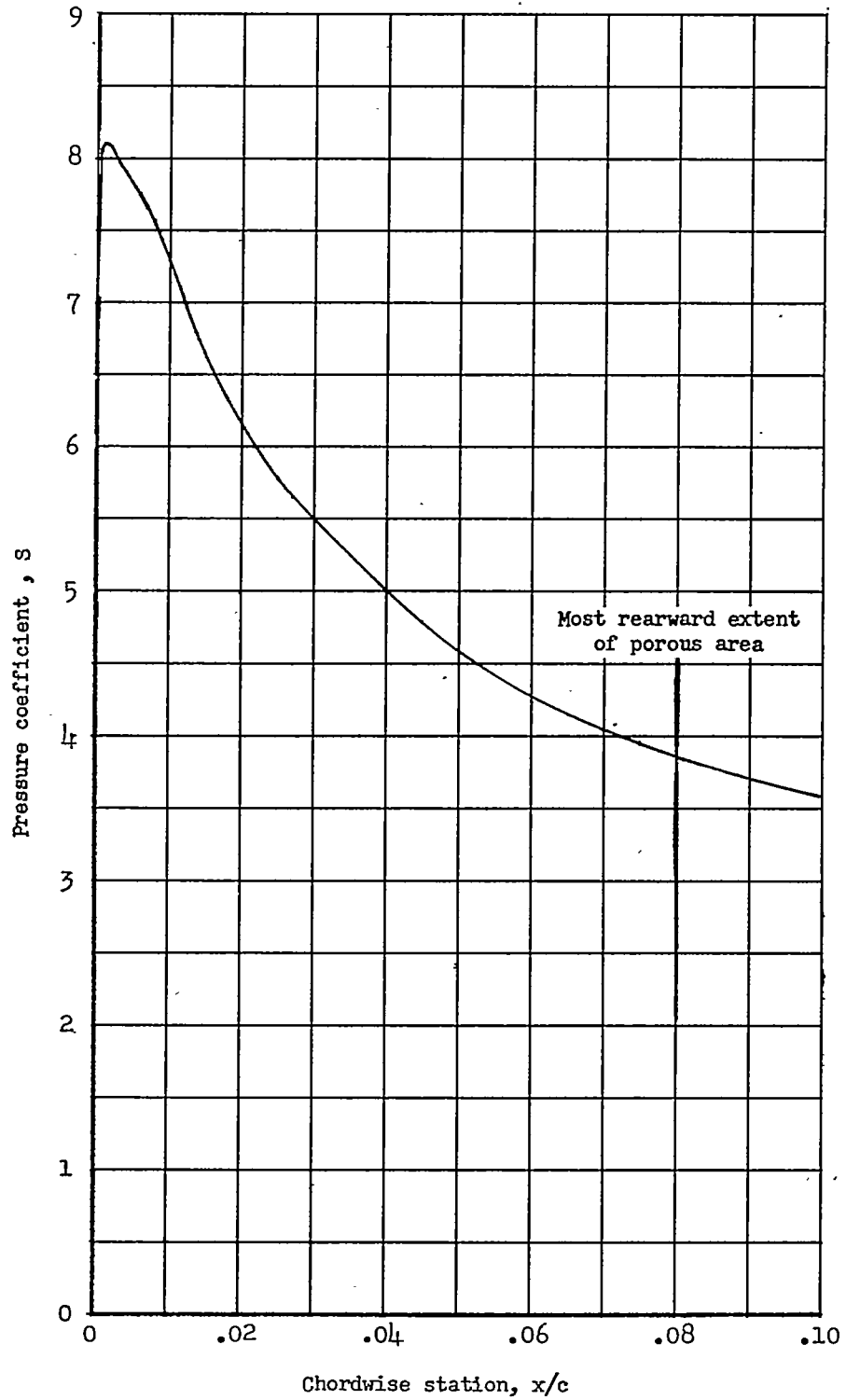


Figure 10.- Theoretical chordwise pressure distribution over the upper surface of the NACA 2412 airfoil at a lift coefficient of 1.6.

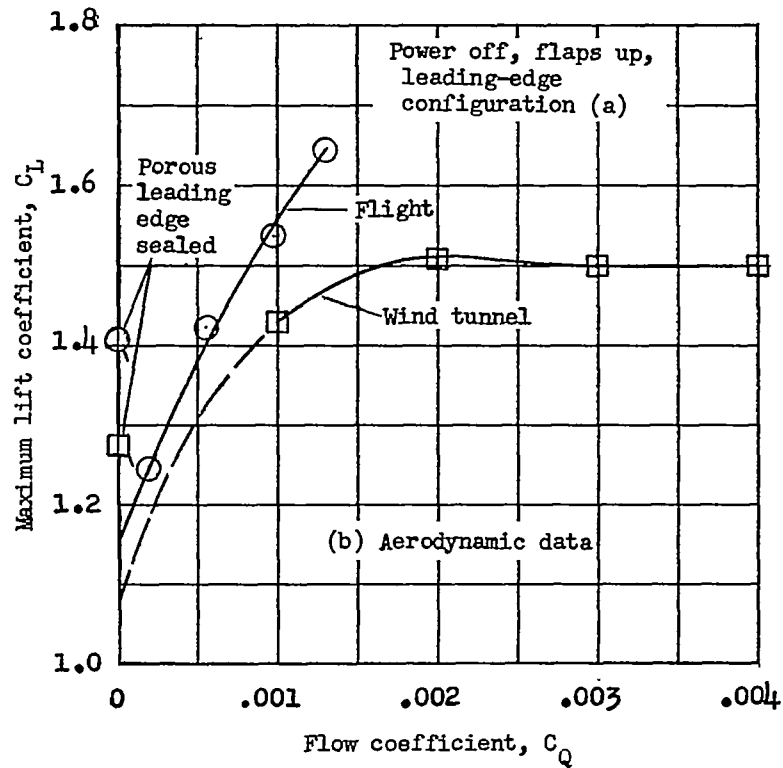
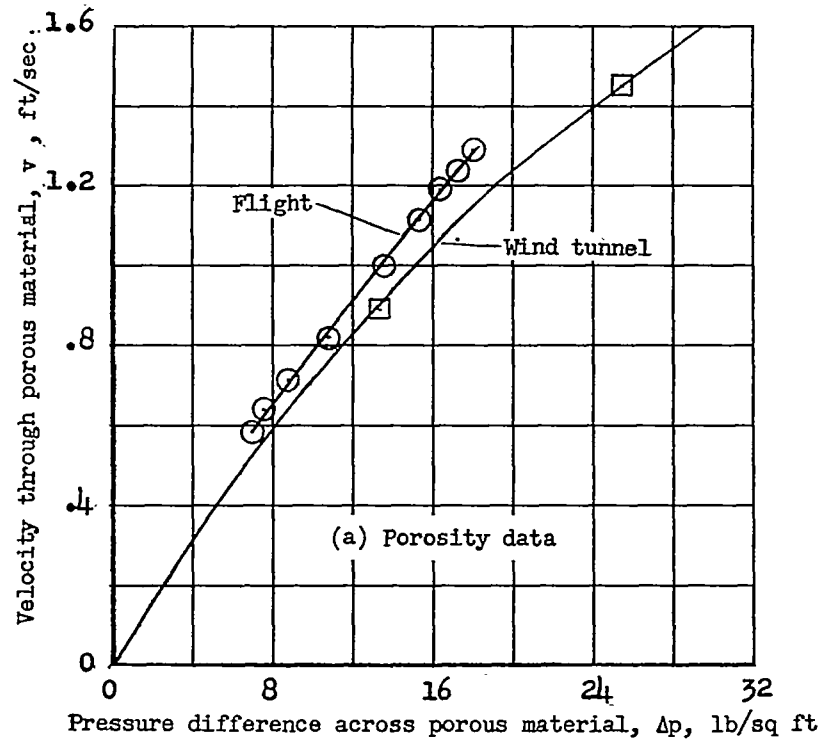


Figure 11.- Comparison of results of flight and wind-tunnel investigations.

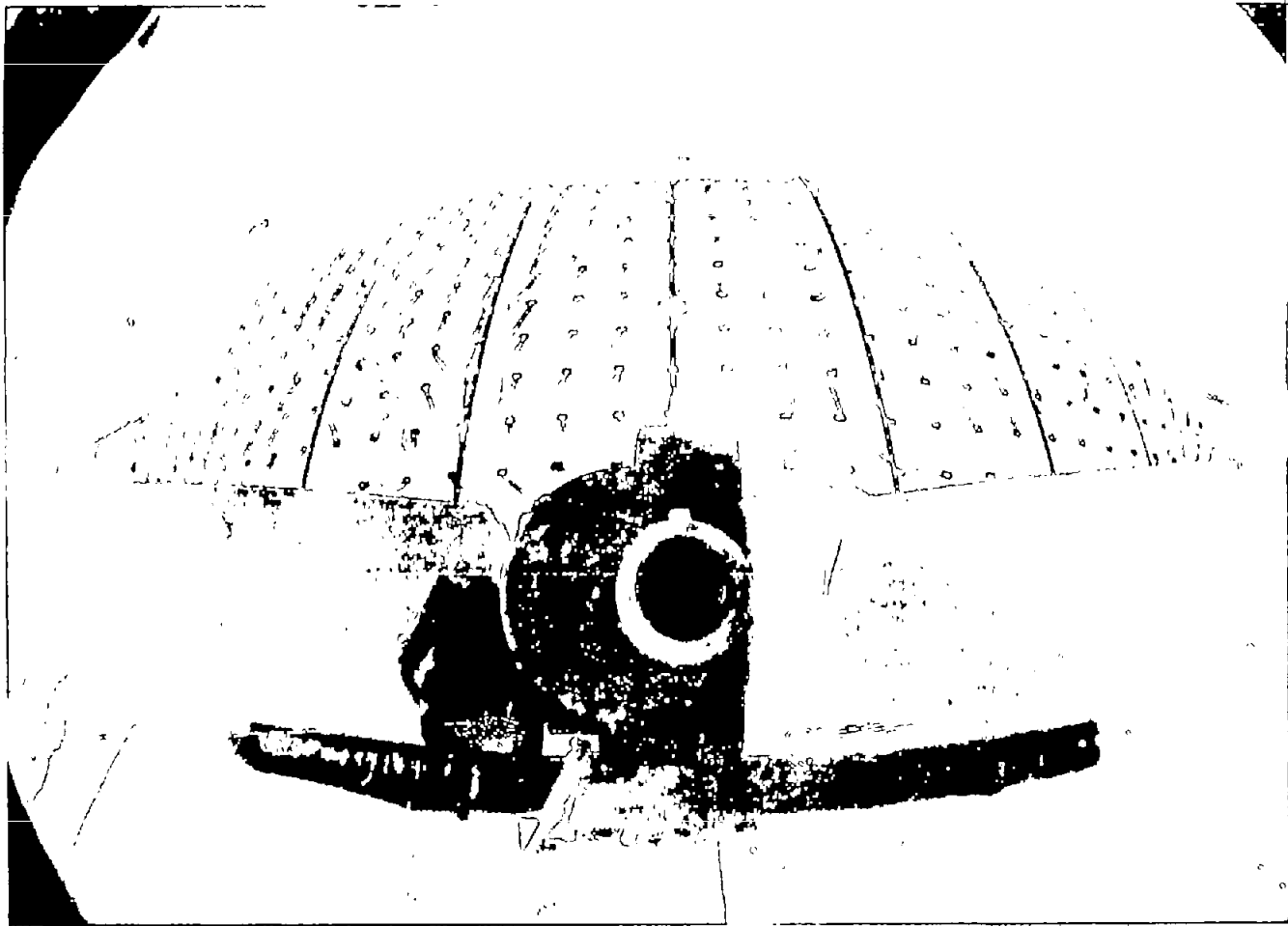


Figure 12.- Typical frame from tuft photographs. L-82055